CHALMERS
UNIVERSITY OF TECHNOLOGY

Textile Reinforced Concrete Structures
Bending tests of one-way slabs

Master's thesis in the Master's Programme Structural Engineering and Building Technology

Ino Blomqvist

Department of Architecture and Civil Engineering
Division of Structural Engineering
Concrete Structures Group
CHALMERS UNIVERSITY OF TECHNOLOGY
Master's Thesis
Gothenburg, Sweden 2021

MASTER'S THESIS

Textile Reinforced Concrete Structures

Bending tests of one-way slabs

Master's Thesis in the Master's Programme Structural Engineering and Building Technology

INO BLOMQVIST

Department of Architecture and Civil Engineering
Division of Structural Engineering
Concrete Structures Group
CHALMERS UNIVERSITY OF TECHNOLOGY
Göteborg, Sweden 2021

Textile Reinforced Concrete Structures
Bending tests of one-way slabs

Master's Thesis in the Master's Programme Structural Engineering and Building Technology

INO BLOMQVIST

Examensarbete
Institutionen för arkitektur och samhällsbyggnadsteknik
Chalmers tekniska högskola, 2021

Department of Architecture and Civil Engineering
Division of Structural Engineering
Concrete Structures Group
Chalmers University of Technology
SE-412 96 Göteborg
Sweden
Telephone: + 46 (0)31-772 1000

Cover:
A carbon fibre reinforced concrete slab after being tested in four-point bending.
Department of Architecture and Civil Engineering
Göteborg, Sweden, 2021

Textile Reinforced Concrete Structures

Bending tests of one-way slabs

Master's thesis in the Master's Programme Structural Engineering and Building Technology

INO BLOMQVIST

Department of Architecture and Civil Engineering
Division of Structural Engineering
Concrete Structures Group
Chalmers University of Technology

ABSTRACT

Textile Reinforced Concrete (TRC) is a promising solution to optimize material use, reduce carbon emissions, and develop new building techniques to reduce the use of finite resources. The possibilities with TRC also include its corrosion-resistance, which prolongs the service life and reduces maintenance needs.

In this thesis, experiments on carbon fibre reinforced one-way concrete slabs were carried out, to study the flexural behaviour in four-point bending tests. The aim of this Master's thesis project was to provide data for further development of modelling methods for TRC and give new insights in the structural behaviour of TRC.

Specimens were produced with two manufacturing methods: clamped mesh and wet lay-up. Two different types of carbon fibre meshes, placed in two different orientations, and combined with two types of concrete were studied. Load-and-deflection relation, maximum load, crack pattern and crack width were studied. To observe and measure the behaviour, Digital Image Correlation (DIC) was used. Thereby the full strain field, and thus the deformations, crack width and crack propagation were measured in detail.

Specimens with type 2 mesh, which was a denser mesh, had a higher load capacity than those with type 1 mesh. The specimens with mesh type 2 also showed a smaller deflection at failure compared to all other specimens, and had a higher stiffness in the cracked stage. Type 1 mesh was tested as both 0° and 45° orientation angle. A brittle failure with rupture of the textile took place in tests with the mesh in 0°, while a slightly more ductile behaviour in form of pull-out of the bundles occurred in tests with the mesh in 45°. The number of cracks in each specimen showed a large variety and better casting quality of the specimen resulted in more cracks. Further, the transverse yarn showed to be a crack initiator for mesh type 1.

The utilization factor of the tensile strength of the textile mesh was on average 0.37 for specimens with 0° orientation mesh, while it was only 0.23 for specimens with 45°. The utilization factor is an important design parameter to consider and improve to make TRC-structures more competitive.

Key words: Textile reinforcements, textile reinforced concrete, TRC, carbon fibre, one-way slab, four-point bending test, DIC, wedge splitting test

Textilarmerade betongkonstruktioner

Böjprovning av plattor

Examensarbete inom mastersprogrammet Konstruktionsteknik och Byggnadsteknologi

INO BLOMQVIST

Institutionen för arkitektur och samhällsbyggnadsteknik
Avdelningen för konstruktionsteknik
Betongbyggnad
Chalmers tekniska högskola

SAMMANFATTNING

Textilarmerad betong (TRC) är en lovande lösning för att optimera materialanvändningen, minska koldioxidutsläpp och utveckla nya byggtekniker för att minska användningen av ändliga resurser. Möjligheterna med TRC avser också dess korrosionsbeständighet i betongkonstruktioner, med andra ord livslängd och underhållsaspekt.

I detta examensarbete utfördes experiment med kolfiberarmerade betongplattor belastade i fyrpunktböjning i en riktning, för att studera beteendet i böjning. Syftet var att tillhandahålla data för vidareutveckling av modelleringsmetoder för TRC och ge nya insikter i dess strukturella beteende.

Prover tillverkades med två tillverkningsmetoder: fastklämt nät och våt uppläggning. Två olika typer av kolfibernät, placerade i två olika riktningar, och kombinerade med två typer av betong studerades. Belastnings- och nedböjningsförhållande, maximal belastning, sprickbildning och sprickvidd studerades. För att observera och mäta beteendet användes Digital Image Correlation (DIC). Därigenom mättes hela töjningsfältet och därmed deformationer, sprickvidd och sprickbildning i detalj.

Provkroppar med typ 2 nät, som var ett tätare nät, hade en högre lastkapacitet än för de med typ 1 nät. Provkroppar med nättyp 2 visade också en mindre nedböjning vid brott jämfört med alla andra prover och en högre styvhet i det spruckna stadiet. Typ 1 nät testades i både 0 ° och 45 ° orienteringsvinkel. Ett sprött brott med avsliten armering inträffade i tester med nätet i 0 °, och ett något mer duktilt beteende i form av utdrag av armeringen inträffade i tester med nätet i 45 °. Antalet sprickor i varje prov visade en stor variation och bättre gjutkvalitet på provkropparna resulterade i fler sprickor. Vidare visade sig de tvärliggande trådarna vara en sprickinitiator för nättyp 1.

Utnyttjandefaktorn för textilnätets draghållfasthet var i genomsnitt 0,37 för prover med nät i 0 ° riktning, medan den endast var 0,23 för prover med 45 °. Utnyttjandefaktorn är en viktig designparameter att beakta och förbättra för att göra TRC-strukturer mer konkurrenskraftiga.

Nyckelord: Textilarmering, textilarmerad betong, TRC, kolfiberarmering, envägsböjning, fyrpunktsböjning, DIC, böjprovning av plattor

Contents

Preface

This Master's thesis work was carried out at the Division of Structural Engineering, Concrete Structures Group, Chalmers University of Technology, Sweden, with Professor Karin Lundgren and Adam Sciegaj as supervisors (Adam during first part of the work).

In parallel to this Master's thesis report another report, "Experimental Study of the Tensile and Pullout Behavior of Textile Reinforced Concrete", has been written by Maarten van Loo; this presents the behaviour of Textile Reinforced Concrete with regard to pull-out and tensile behaviour. These two reports are both part of an ongoing research project at Chalmers concerning Textile Reinforced Concrete.

The experiments in this Master's thesis work was performed during early spring 2020, in the Structures Laboratory, at Chalmers University of Technology together with Maarten van Loo and with support from Sebastian Almfeldt. The results from the experiments were analysed in the computer software DIC, with supervision from Mathias Flansbjer.

I would like to thank Sebastian, Adam and Mathias for their help, commitment and supervision. I would also like to thank StoCrete that donated textile reinforcement and concrete to use in the experiments. Finally, I would like to especially thank Karin and Maarten for your support during the project.

Göteborg June 2021

Ino Blomqvist

1 Introduction

1.1 Background

The environment is a hot topic today in all fields in society. The global warming does not only mean an increase of temperature but also implicates an increasing amount of natural disasters and a rise of the sea level which affects coastal communities. The global warming is argued to be a consequence of the high amount of greenhouse gas emissions since the beginning of the industrialism. Another effect on the environment that the industrialism led to is the use of finite resources.

One of the biggest influencers on the environment is the building industry. The production of buildings, including manufacture and transportation of building materials and the construction process, stands for about 11% of the greenhouse gas emissions (Budds, 2019). The building industry also accounts for about 40% of the materials used globally (Roodman & Lenssen, 1995; UNEP, 2009) and many building materials come from finite resources such as clay, sand and coal.

1.2 Problem discussion

Due to climate changes the building industry strives for optimization of materials and reduced carbon emissions from production. It is of major interest to search for and develop new building techniques and combine different materials so that we can reduce the amount of used material.

As an alternative to traditional construction materials and methods, Textile Reinforced Concrete (TRC) makes it possible to build slender freeform light weight structures. A slender concrete structure means less material and less amount of emissions than a non-slender concrete structure, hence TRC-structures have a relatively small environmental impact. Also, slender freeform light weight structures are of big interest not only to architects but also from the structural optimization point of view.

The possibilities with TRC are not only aesthetic, structural or environmental, but also concern the lifespan and maintenance, or in other words the corrosion-resistance aspect of concrete structures. Corrosion of reinforcing bars is one of the biggest issues for conventional building methods and reinforcement that cannot corrode can prolong the lifetime of a structure.

TRC can be used for both new structures and strengthening of existing structures. Compared to traditionally reinforced concrete structures, TRC resembles a combination of traditional reinforcement as well as fibre reinforced concrete with fibres distributed in the concrete matrix. The fibres in TRC are bundled together and can be positioned considering the principal loading direction. Compared to other methods of fibre reinforced concrete, this gives more effective use of the fibres and it also resembles the use of traditional reinforcement. In other words, TRC combines the benefits of both traditional reinforcement and fibre reinforced concrete and can be a possible environmental friendly and optimized option for building in the future.

There are many different materials like glass, textile and other polymers that have been used as reinforcement. This thesis focuses on carbon fibres.

1.3 Aim and objective

This Master's thesis work was part of a research program called "Multiscale modelling of textile reinforced concrete structure" at the Department of Civil and Environmental Engineering, Chalmers University of Technology. The research program aims to develop a multiscale modelling framework for textile reinforced concrete structures and focuses of the execution of the experimental part.

The aim of this Master's thesis project was to provide data for further development of modelling methods for TRC and give new insights in the structural behaviour of TRC. The main objective was to through experiments provide data for future use to develop better and more accurate modelling methods, to characterize and understand the structural behaviour of TRC and hence improve the understanding of the behaviour of TRC. Furthermore, the objectives were to describe the load-and-deflection relation under four-point loading on plates with varying reinforcement orientation as well as to describe deformation, maximum load and study the crack pattern. Experiments were conducted to study the flexural behaviour on one-way slabs with four-point bending tests. The results of the experiments were analysed and compiled to provide data for future use. Different textiles and types of concrete were studied in this master's thesis as well as how to produce, plan and execute the tests.

This Master's thesis was a continuation of the Bachelor's thesis by Delibasic and Hayatleh (2019) and was a resumption and development with new experiments. The experimental work of this thesis was done in parallel with experimental work of another thesis; the results of that work can be found in van Loo (2020).

1.4 Limitations and adjustments

The experiments were planned to consist of four-point bending tests on TRC plates, both on slabs (lying) and on deep beams (standing). However, during first casting of the samples, the concrete was not flowable enough, which led to that quite a number of specimens had to be discarded. The many damaged samples led to an adjustment in aim and limitations of this thesis. Thus, two more specimens were produced with a different mesh and a different production method.

Different orientations and placement of the mesh were studied. The structural behaviour, such as crack development, loading, deformations and strains was studied, analysed and compiled.

This thesis focuses on two types of carbon reinforcement mesh and two different types of concrete, which is described in Chapter 3. One geometry of the slabs was considered, with an exception for thickness where samples with two layers of reinforcement was studied. Further, only four-point bending for one-way slabs were tested.

1.5 Methodology

The Master's thesis work started with a literature study to obtain knowledge about the known behaviour of textile reinforced concrete in previous experimental studies. The literature study also aimed to investigate how previous experiments on textile reinforced concrete were conducted and to plan for tests similar to those.

The second part of the Master's thesis work was to perform experimental studies, to investigate the structural behaviour of textile reinforced concrete. The experimental studies began with preparations such as building formworks and casting the samples. The test set-ups for the experiments are described in Chapter 3 and the results from the experimental study can be found in Chapter 4.

In order to achieve the previously specified aim, it is necessary to reflect the real structural behaviour in the experiments in the best possible way. The TRC specimens were designed and produced in the Structures Lab at Chalmers University of Technology. Investigation of existing reports of experiments were conducted to be able to draw conclusions of the best way to produce the test specimens. After the dimensions of the specimens were decided, frameworks were constructed and concrete matrix was mixed. All the specimens with the first type of reinforcement were manufactured at the same time with the same concrete properties and conditions. However, the two extra specimens with the second type of reinforcement were cast later but still in the same premises.

The tests were executed in the lab and the equipment used provided data on phenomena such as crack patterns and crack distribution, deflections and strains in the material. To observe and measure the behaviour Digital Image Correlation (DIC) were used. Thereby the full strain field, and thus the deformations, crack width and propagation were measured in detail.

Also wedge splitting tests and compression tests for the plain concrete were conducted.

2 State of the art

2.1 Textile reinforced concrete structures

Historically humans have used fibre reinforcement in building materials for thousands of years. It has been found that brittle materials like bricks have been reinforced with vegetable fibres and animal hairs. In modern times one well known fibre reinforcement is asbestos fibres, which is now abandoned in construction due to health issues. For the latest 40 years, there has been an increasing interest in developing different cement-based products with fibre reinforcement. Some main reasons for developing new techniques are cost efficiency, sustainability and ecology.

The most commonly used material in conventional reinforced concrete (RC) is steel. Steel bars are relatively easy to use and have advantages regarding safety in its ductile behaviour. However, there are disadvantages with steel in terms of corrosion and hence high maintenance costs in such structures.

Another technique is fibre reinforced concrete, or FRC, which uses short fibres randomly distributed within the concrete mixture. This lowers the labour required and creates possibilities of more freeform structures. However, it is very difficult to spread the fibres evenly within the concrete, some parts of the structure may contain more fibres and some may contain less. This makes it more difficult to predict the structural behaviour and makes it unreliable.

A third technique is textile reinforced concrete, or TRC, which this master's thesis is focusing on. TRC takes advantages of both before mentioned techniques. The orientation of the textile reinforcement can be placed in a controlled way and even be placed more efficiently in a desired position which saves material. Also, the materials do not corrode so it eliminates one of the problems with steel bars, hence lots of concrete could be saved due to less cover thickness. The smaller thickness also allows thinner structures and the flexibility of the fibres allows freeform shapes. The possibilities are not only aesthetic or structural but concern also corrosion-resistance aspect of concrete structures, which is one of the biggest issues for conventional building methods and can improve the lifetime and maintenance of the structure and lower the overall costs. **Fig 2.1** shows the principle of these three techniques.

Compared to traditionally reinforced concrete structures, TRC resembles a combination of traditional rebar reinforcement as well as fibre reinforced concrete with fibres distributed in the concrete matrix. The fibres in TRC are long and continuous, called filaments. They are bundled together and can be positioned considering the principal loading direction. Compared to other methods of fibre reinforced concrete, this gives more effective use of the fibres; it also resembles the use of traditional reinforcement. In other words, TRC combines the benefits of both traditional reinforcement and fibre reinforced concrete and can be a possible environmental friendly and optimized option for buildings in the future.

Textile reinforcement consists of woven nets of multiple threads bundled together often with glue. The textile reinforcement available on the market today mostly consists of two-dimensional open textile meshes with 1-5 cm spacing. This mesh is then combined with fine grain concrete.

The size of the mesh limits the maximum size of the aggregate hence textile reinforcement is used with concrete with aggregate size around 2-4 mm (Brameshuber, 2006). It is of high importance that the concrete is chemically

compatible with the textile reinforcement, why low alkalic concrete is preferable. Another issue to fully utilize the reinforcement is that the concrete flows properly in between the meshes. Due to the formation of the textile reinforcement the surrounding concrete can only penetrate the outer filaments but not the core. This means that filaments can slip versus each other, forces are transferred through friction between the filaments. Hence it is not possible to fully utilize the full tensile strength of the fibres, which is why it is reduced with coefficients in design. Factors affecting these coefficients are for instance the size of bundles (sizing), impregnations, epoxy or manufacturing technique.

Textile reinforcement is brittle and has very little plastic deformation and cannot carry loads in compression. To develop new cement-based composites manufacturing technique must be developed to increase efficiency, as well as experimental characterization techniques and modelling of the interaction between concrete and fibres. For instance, modifications in shapes of the fibres and improving the fibre-matrix bond are ways of improving the utilization factor. To continue the application of TRC further investigations are needed to develop simple and reliable calculation methods for strength, stiffness, and durability.

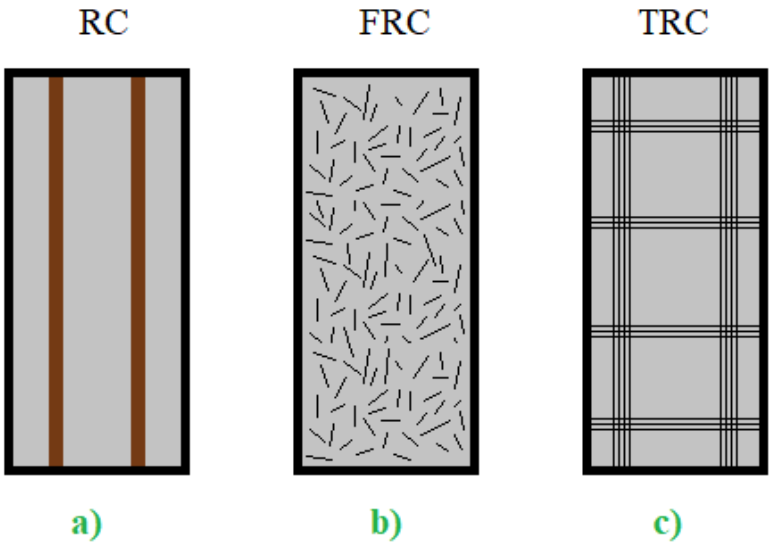

Fig 2.1: *Principles of reinforcement techniques, a) Rebar Composite, b) Fibre Reinforced Composite, c) Textile Reinforced Composite.*

2.2 Flexural behaviour of one-way slabs

The mechanical properties of textile reinforcement depends on fibre material, roving size and binding type, and goes even further in range with the addition of epoxy and impregnated yarns. Thus, a division of impregnated and unimpregnated yarns has to be done when dimensioning TRC structures. The bearing capacity is mostly affected by the mentioned characteristics of the textile reinforcement but also the cross-section area of the yarns which can be described by the weight per length, often in units grams per kilometre. The purpose of impregnation is to achieve a homogenous stress profile of the bundle of yarns which will lead to a better activation of the inner filaments and hence higher strength (Triantafillou, 2016).

For straight beams and slab elements impregnated fabrics is most commonly used. This type of structural element can be described as simply supported one-way slab for which the Ultimate Limit State (ULS) can be calculated based on a priori known critical cross-section. An example of this is façade panels attached to the loadbearing structure of a building, which in this particular case has two stiffening ribs goes vertically along the panel. The horizontal wind loads acts on the panel and is carried by the panel as a one-way slab in between the ribs. Hence the dimensioning can be done by modelling a simply supported slab element with rectangular TRC cross-section with an assumed linear strain distribution, a similar approach as to steel-reinforced structures. Experimental results have shown to comply fairly well with the predicted calculated values with a scatter of about 5% (Triantafillou, 2016).

The most common method of experiments on TRC is by four-point bending tests with slabs and beams in varying sizes in order to determine the flexural behaviour. The reinforcement consists of non-corrosive fibre grid, or open mesh structure. In comparison to FRC a mesh grid can spread the energy over the entire specimen which gives a homogeneous microcracking state. Tests shows that the flexural behaviour of TRC is initially linear elastic but early microcracks form and propagate. Where the first crack appears is not predetermined if the specimens are not notched and the deformation is dominated by the crack propagation (Mobasher, 2012).

Textile reinforcement has a linear elastic behaviour under tensile loading. The fibres are also very brittle and have a sudden failure when reaching ultimate stress. But even if the material has no plastic capacity, slippage of individual yarns in the heterogenous structure gives an uneven pull-out which leads to a somewhat ductile behaviour.

In a previous work by Portal et al. (2015), one-way slabs with dimensions 1000×200×50 with one layer of reinforcement were tested. Similar dimensions were chosen for the specimens in this report. Portal described the flexural behaviour of her one-way slabs with carbon reinforcement by four states. State I for uncracked concrete, State IIA for crack formation, State IIB for crack stabilization, and State II for failure. Further, there was delayed load distribution in form of a load drop that probably is dependent on the geometric waviness of the fabric (Portal et al. 2015). It was also found that a stabilization of the crack formation occurred in State IIb in form of a gain of stiffness, or strain hardening, which also depended on the textile reinforcement properties.

Hegger and Voss (2008) have tested beams with a length of 1m in deformation-controlled four-point bending tests. They found that the carbon reinforcement yielded higher strength in bending than in tensile tests, which could be explained by the pressure from the deflection (Hegger and Voss, 2008). They also found a correlation between the calculated ultimate strength and the reinforcement ratio. As for traditional reinforced concrete, the calculated capacity in bending depends on the reinforcement's tensile strength and the internal lever arm, but unlike traditional steel, for TRC the capacity in bending also depends on the bond properties between the textile and concrete. Therefore, parameters such as the geometrics of the rovings and filaments influence.

2.3 Cracking

Due to the low tensile strength in concrete, cracking is inevitable in such structures. One of the most common issues due to cracking is corrosion of the steel reinforcement, which requires high maintenance and repairs.

TRC composites have a different crack pattern compared to conventional reinforced concrete, where rebars gives fewer but larger cracks, i.e. TRC have more cracks but smaller. This affects the maintenance aspect of a structure. Carbon fibres can increase the strength and stabilize the microcracks in fibre reinforced composites (Mobasher, 2012). Carbon fibres are bonded together in microcrystals that are aligned parallel to the fibres longitudinal axis and makes it very strong which makes it an interesting substitute to steel. Beside the strength, other important properties for structural applications are stiffness, strain capacity, and resistance to crack growth.

3 Experiments

3.1 Overview

In this Master's thesis four-point bending tests on TRC plates were executed, thus tested as one-way slabs. A total of 11 specimens were tested; an overview can be seen in **Table 3.1**. The specimen's dimensions were 900×200×20 (mm) for slabs with one layer of reinforcement mesh and 900×200×30 (mm) for slabs with two layers. The slabs with two layers of reinforcement were made thicker to ensure that the reinforcement was located in the tension zone.

The mesh was placed 5mm from the bottom and in the case with two layers there were also 5 mm in between the meshes, see **Fig. 3.1**. The specimens with mesh type 1 contained 5 bundles along and 23 bundles across, while mesh type 2 had 20 bundles along and 112 bundles across. The mesh type 1 was also oriented in two different ways, 0° and 45° angle, see **Fig. 3.2**. The specimens were named with 'S' for slab followed by a number indicating the number of layers of reinforcement, then a number of 45 when angled mesh, and lastly the number of the specimen. For instance 'S2-45-3' is a slab with 2 layers of reinforcement in a 45° orientation and is the 3:rd specimen of this type.

Table 3.1: *Overview of experimental program*

Specimen	Thickness [mm]	Concrete	Type of mesh	Layers	Angle [°]	Production method
S1-2	20 mm	StoCrete	type 1	1	0	1 Clamped mesh
S1-3	20 mm	StoCrete	type 1	1	0	1 Clamped mesh
S1-4	20 mm	StoCrete	type 1	1	0	1 Clamped mesh
S1-45-1	20 mm	StoCrete	type 1	1	45	1 Clamped mesh
S1-45-3	20 mm	StoCrete	type 1	1	45	1 Clamped mesh
S2-45-3	30 mm	StoCrete	type 1	2	45	1 Clamped mesh
S2-45-4	30 mm	StoCrete	type 1	2	45	1 Clamped mesh
S1-T1	20 mm	StoCrete	type 2	1	0	2 Wet lay-up
S1-T2	20 mm	AAS	type 2	1	0	2 Wet lay-up

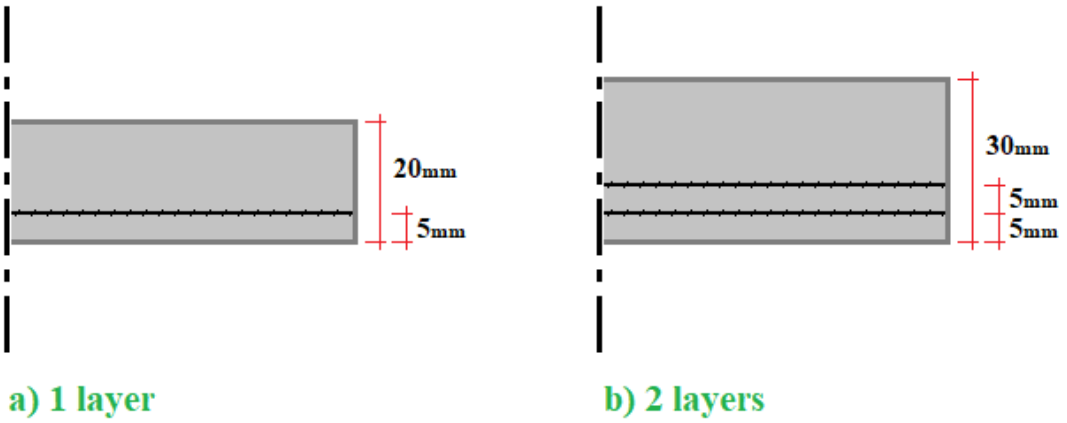

Fig 3.1: Cross-section of the specimens: a) with 1 layer, b) with 2 layers.

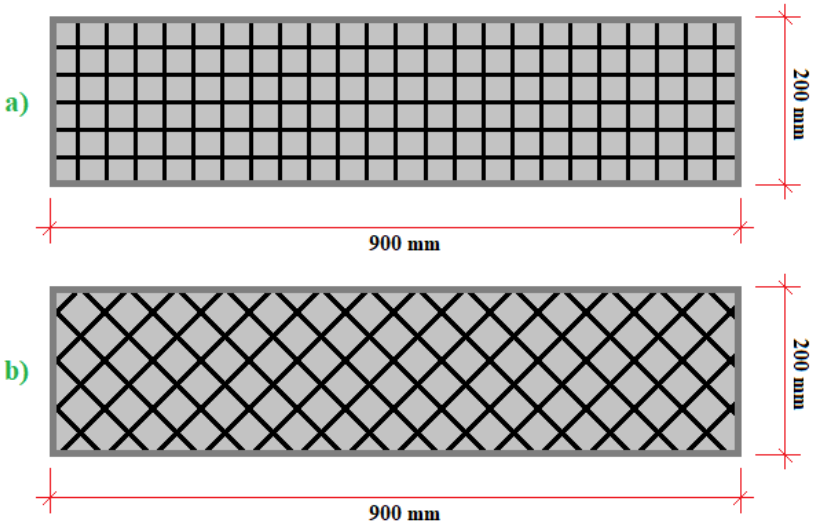

Fig 3.2: Sketch of mesh orientation: a) with 0°, b) with 45°.

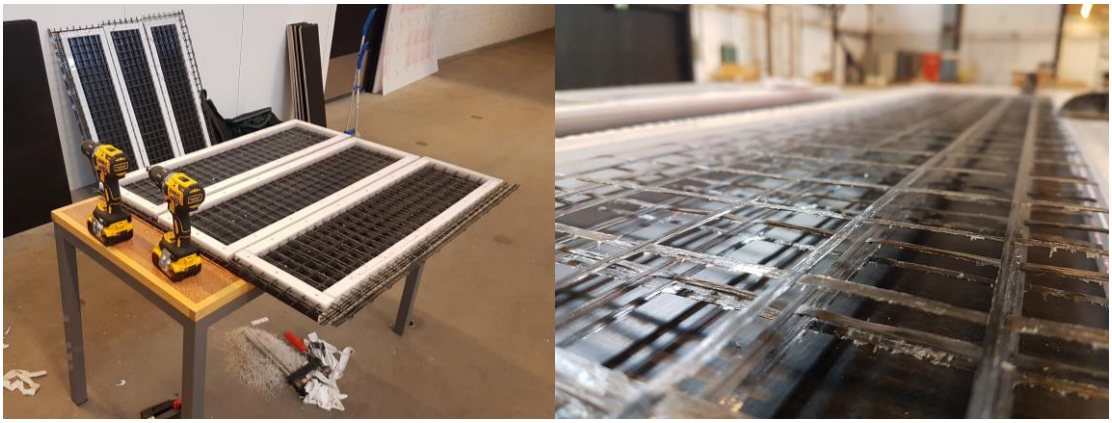

Fig 3.3: Photos of the production of clamped mesh frames.

3.2 Production and adjustments

The specimen's dimensions were chosen similar to earlier work (Portal et al. 2015). Two production methods were used: Method 1 with clamped mesh, and Method 2 with wet lay-up.

In the first production method, the framework was produced by 5 mm plastic pieces screwed together. The reinforcement mesh was clamped together in between the pieces to make it stay in the right place, and in the case with two layers the second layer of mesh was clamped in between the next pieces of plastic, see **Fig 3.4**.

In the second production method, with wet lay-up, the framework was built with a wooden frame. Concrete was poured up to 5 mm thickness, thereafter the reinforcement mesh was placed, and finally the rest of the concrete was poured, see **Fig 3.4**. Two specimens were produced in this way, and they also differed in the sense that they contained a different reinforcement mesh.

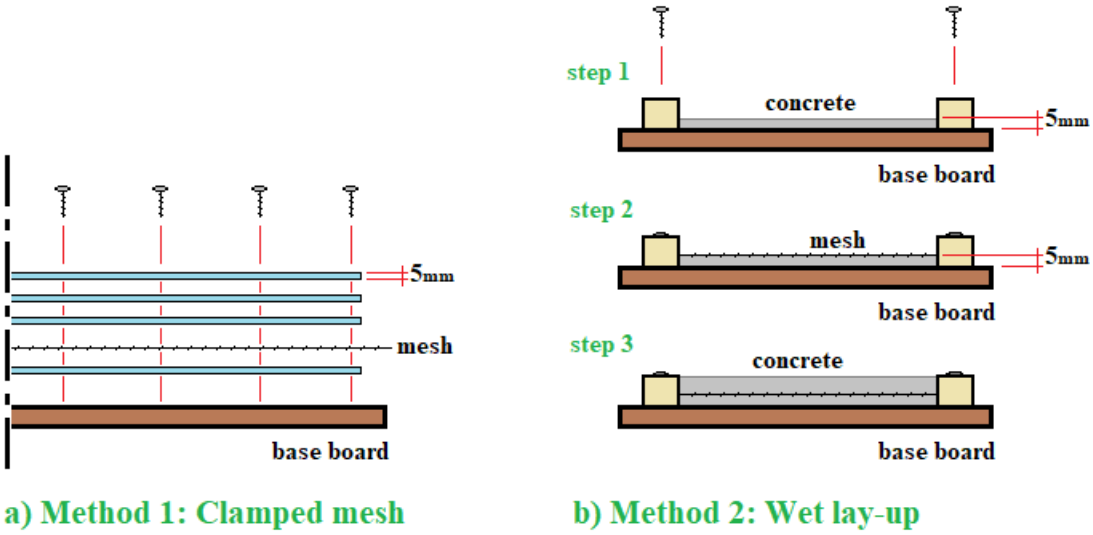

Fig 3.4: *Sketch of production methods: a) Method 1: Clamped mesh, b) Method 2: Wet lay-up.*

After casting, all specimens were stored and hardened under plastic foil and were moisturized every 2 to 3 days to prevent them from drying out. The specimens were removed from their framework after 21 days, and the actual tests were conducted after a curing period of 28 ± 2 days. The material tests were conducted first, followed by the four-point bending tests.

During casting of the samples using the first production method, there were problems with the concrete not being flowable enough. The concrete was mixed in two batches; at mixing of the second batch, plasticizer was added to make the concrete more flowable. In the samples that were cast with the first thicker concrete mix the concrete had not fully flowed out and covered the reinforcement, see **Fig. 3.5**. This was noted first when the samples were taken from the formwork and the bottom of the specimens could be seen. Therefore, all the specimens produced with the first concrete batch were discarded, which unfortunately led to a reduction in numbers of slabs tested and that no tests on deep beams could be carried out as initially intended.

Thus, the many damaged samples led to an adjustment in aim and limitations of this thesis. However, two of the discarded specimens were picked and used to adjust and practice the set-up for the experiments.

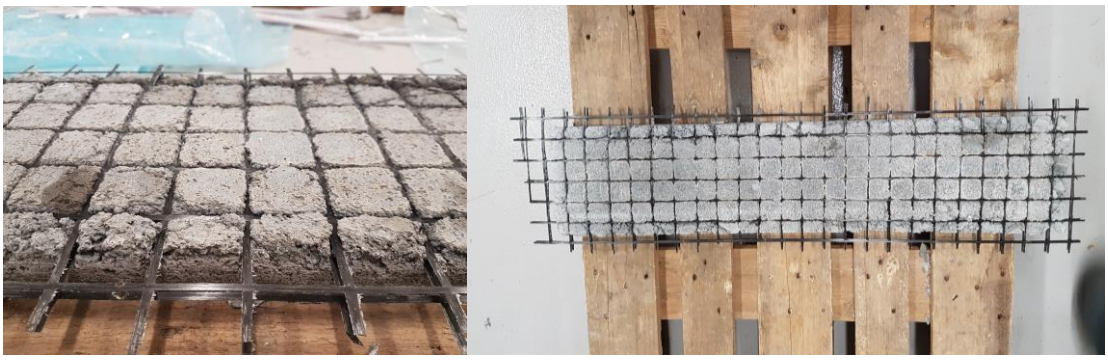

Fig 3.5: *Photos of one of the discarded specimens.*

3.3 Four-point bending test set-up

The four-point bending tests were conducted in a rig constructed and designed for this experiment. Measurements and distances were determined after previous similar experiments by Portal et al. (2015). The 50 mm distance from the edge of the slab to the support was chosen to ensure anchorage and that the slab would stay on the support even during large deflections. The set-up is shown in detail in **Figs 3.6-7**.

The rig was custom made for these experiments with special supports. The supports were cylinder rollers so that the slab could move freely as simply supported. Shelves were also added to prevent pieces from the specimens to fall down and damage the equipment. The tests were carried out in deformation control: a loading rate of 3 mm/min for the deformation of the hydraulic jack was used.

The test were executed up-side down relative normal loading conditions. This was to be able to rig the cameras for the Digital Image Correlation (DIC). It was easier to install the cameras to see well from above and it was also a good way to protect the camera equipment from falling parts.

Digital image correlation, or DIC, is used in experiments to measure deformations in structures using a high number of pictures and tracking the movement during the test. To be able to track the movement, a pattern of small dots with high contrast were painted on the specimens, see **Fig 3.8**. Images were acquired during testing at a rate of 1/10 Hz. An ARAMIS® adjustable stereo camera system was used, see GOM (2021a). The results were subsequently processed by the software GOM® Correlate (GOM2021b).

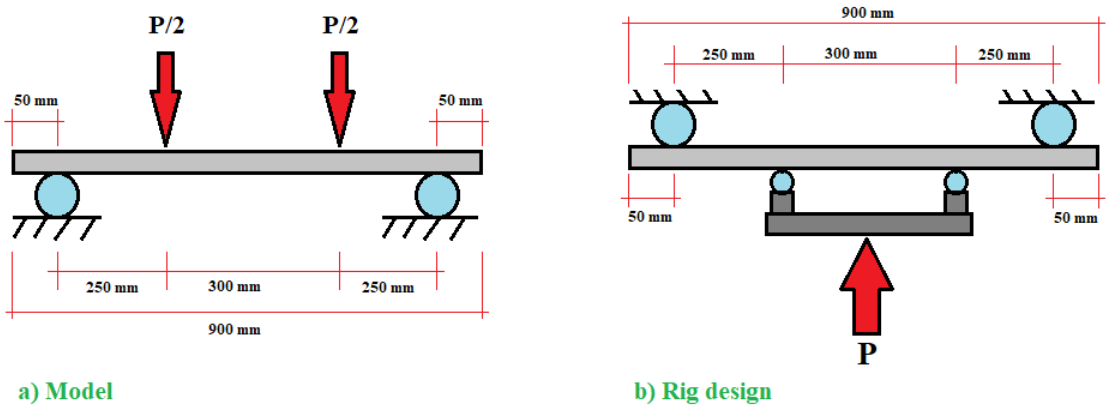

Fig 3.6: *Sketch of test set-up, a) Design model, b) Rig design.*

Fig 3.7: *Photos of the rig and test set-up.*

Fig 3.8: *Photos of the dotted pattern painted on the specimens.*

3.4 Material

Two types of concrete were used. For 10 of the slabs, the concrete was StoCrete R 40-3 mm. The concrete was cast according to the instructions on the package, except for an addition of plasticizer to make the concrete more flowable. Thus, the StoCrete concrete was produced using 2.7 L of water and 40 mL of super plasticizer for each 25 kg bag of concrete. (As described in section 3.2, the concrete in a first batch was too thick, and all specimens produced with that batch had to be discarded. Thus, they are not described further in this thesis.) Specifications of the concrete can be found in **Table 3.2**. The characteristics of the concrete were determined using both compression and wedge splitting tests. The compressive strength of the concrete according to the package was C30/37. The actual compressive strength can be found in Chapter 4. The second type of concrete was a mortar using alkali-activated binder. The mixture proportions of this concrete can be found in **Table 3.3**.

There were also two types of reinforcement used. For 9 of the slabs, the reinforcement was StoFRP Grid 1000 C 390. This mesh has a Young's modulus of 242 GPa and a tensile strength of 5500 N per yarn, according to the technical documentation provided by the manufacturer. Specifications of the reinforcement can be found in **Table 3.4**.

The second mesh was another carbon fibre mesh with mesh size 10 mm, including warp 4 mm and space 6 mm (with 12k filaments/fibres per yarn), by 8 mm including weft 3 mm and space 5 mm (with 6k filaments/fibres per yarn), see **Fig 3.9**. The original mesh was sized with water soluble agent and impregnated with nano-C-S-H (calcium silicate hydrates) by a newly developed technique by L. Tang (under patent process).

Table 3.2: *Technical specifications of StoCrete R40-3 mm.*

Density ρ	Compression strength f_{ck}	Young's modulus E	Max grain size
2257 kg/m^2	> 45 MPa	≥ 20 GPa	3 mm

Table 3.3: *Mixture proportions of self-made alkali-activated mortar.*

Cement (CEM II/A-V 52,5 N)	GGBF slag (Merit 5000)	Gypsum	Sand (0-2 mm)	Activator (water glass, n=1.0, solid content 19.6 wt%)
100	400	20	1560	323.4

Table 3.4: *Technical specifications of StoFRP Grid 1000 C 390.*

Density ρ	Tensile strength	Young's modulus E	Fracture elongation ε	Thickness	Mesh opening
390 g/m^2	5500 N/yarn	242 GPa	17 ‰	1.2 mm	± 390 mm

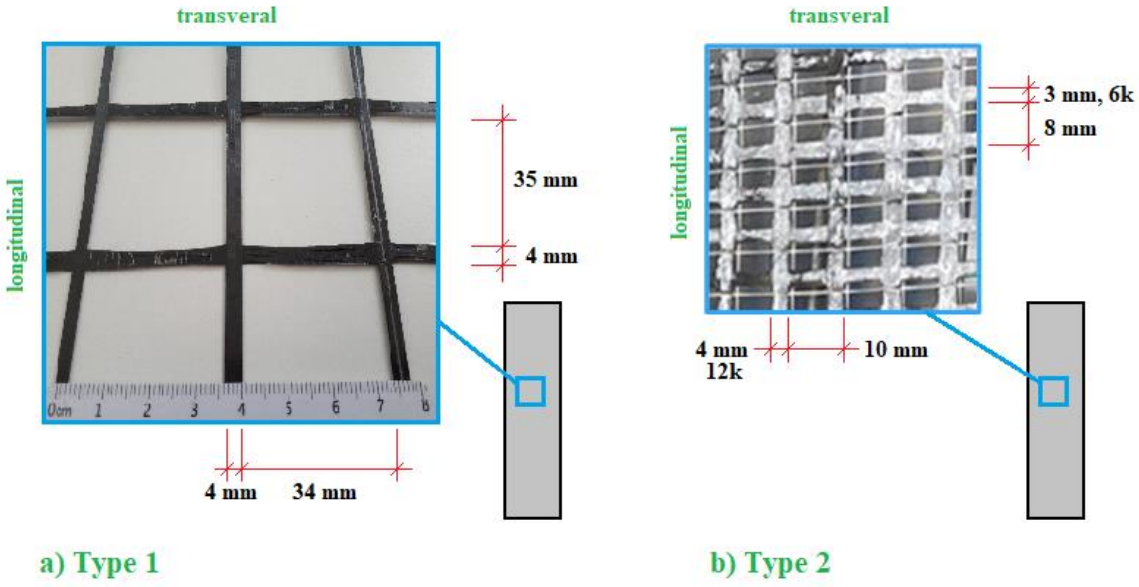

Fig 3.9: *Measurements of mesh, a) Type1, b) Type 2.*

Fig 3.10: *Photo of StoCrete R40 3mm.*

3.5 Material tests (C, WST)

Compression tests were conducted, and the stress and strain relation from these can be seen in **Fig 3.11**. Specimens C1A, C1C and C2A were similar in failure and resulted in a satisfactory failure pattern, see **Fig 3.12**. As can be seen in the graph in **Fig 3.11**, specimen C1B differed from the others; this specimen was deemed not valid according to SS-EN 12390-3:2019 in terms of its unsatisfactory crack pattern.

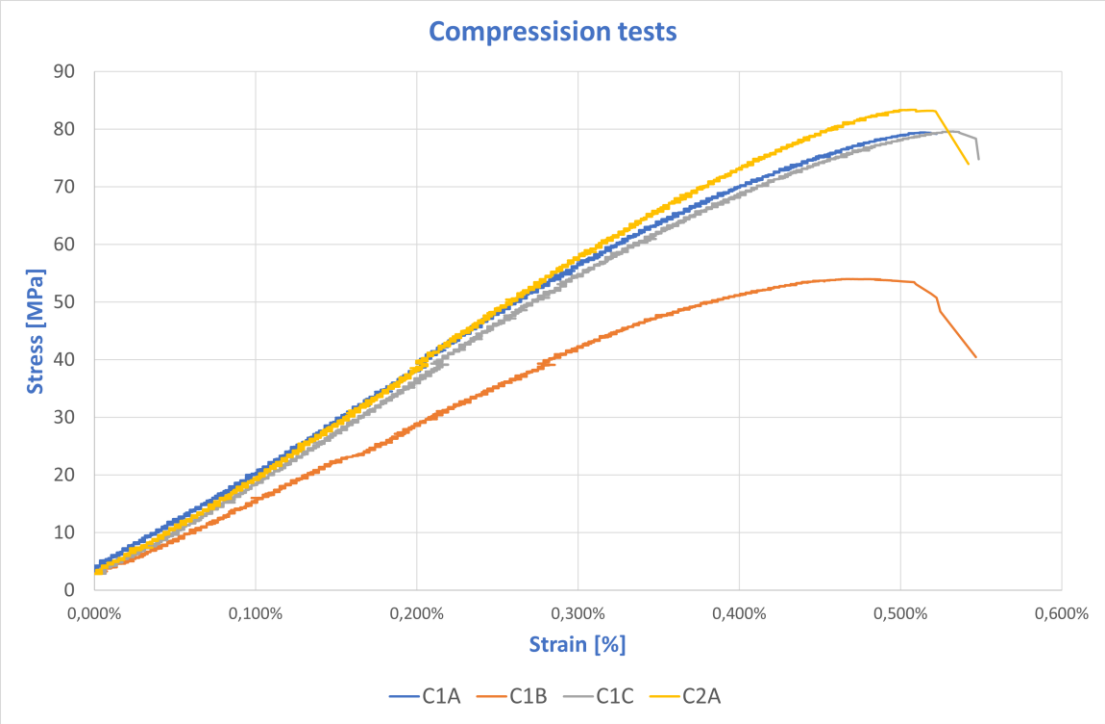

Fig 3.11: *Stress and strain relation of concrete compression tests.*

Fig 3.12: *Photo of crack pattern from compression test.*

The results in terms of maximum compression stress can be seen in **Table 3.5**, with **μ** as the average value of the maximum force, and **S'** is the standard deviation for a sample. The maximum stress values exceeded the ones stated by the manufacturer. Also, there was no significant difference between specimens with superplasticizers and without.

Table 3.5: *Results from compression tests.*

Specimen	Maximum force [kN]	Maximum stress f_{cm} [MPa]
C1A	633.9	79.4
C1B*	424.0	54.0
C1C	625.2	79.6
C2A	654.8	83.4
μ	634.6	80.8
S'	17.5	2.2

**excluded from results.*

The wedge splitting test is an alternate method to 3-point bending test to measure tensile stress and fracture energy. Wedge splitting test specimens consist of cubes (or cylinders) with a groove and a cut notch, see **Fig 3.13**. At testing, a force is applied transversally with a wedge in between rollers. Wedge splitting test is widely used in research to analyse the mechanical behaviour of fibre reinforced concrete and has a lot of benefits compared to 3-point bending tests: smaller size and different shapes can be used. In this work, wedge splitting test on cubes were conducted.

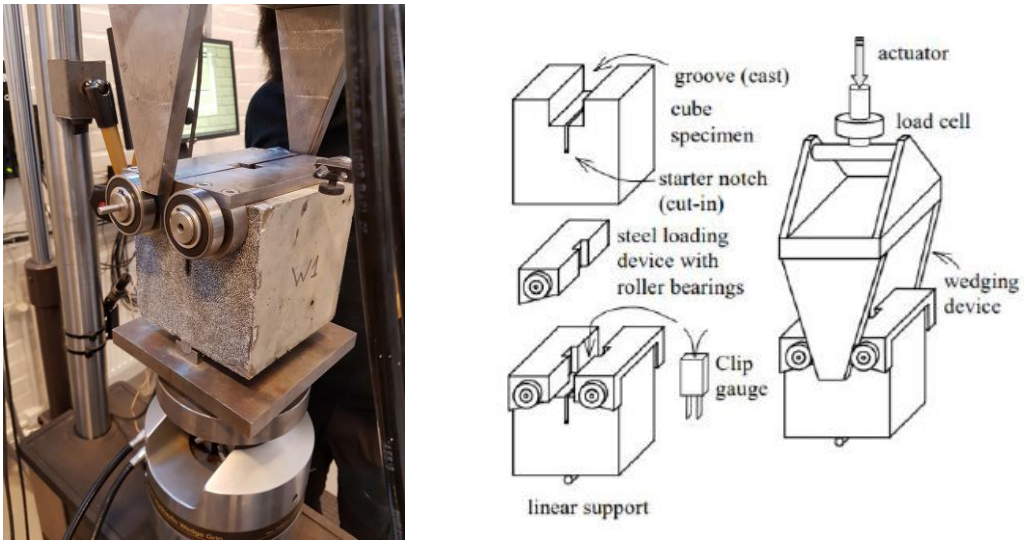

Fig 3.13: *Photo and description of wedge splitting test.*

Wedge splitting tests were conducted, and the results can be seen in **Table 3.6**, with **μ** as the average value of tensile strength of the concrete, and **S'** is the standard deviation for a sample. DIC was also used in these tests and **Fig 3.14** shows the crack pattern. Specimen WST W3 unfortunately cracked during the set-up and those values are therefore considered not valid.

Table 3.6: *Results from wedge splitting tests.*

Specimen	Maximum force [N]	Tensile strength [MPa]
WST W1	2202,0	3,64
WST W2	1981,2	3,28
WST W3*	371,9	0,62
μ	2091,6	3,46
S'	156,1	0,25

**excluded from results.*

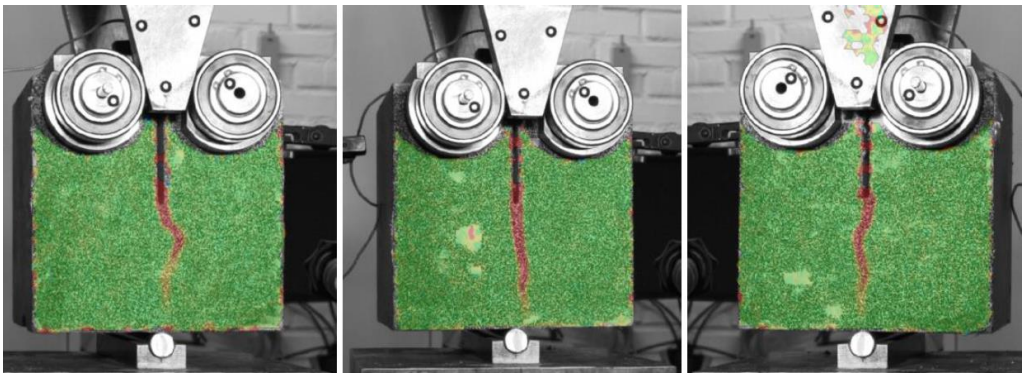

Fig 3.14: *Photo of crack pattern from wedge splitting tests, WST W1 (left), WST W2 (middle), and WST W3 (right).*

4 Results

4.1 Overview

This chapter shows an overview of the results from the four-point bending tests in the form of load versus deflection graphs. Results for each specific specimen is presented in respective chapters. The deflection was evaluated from the DIC results as the mid-point deflection relative to the deflection at the point loads, see **Fig 4.1**.

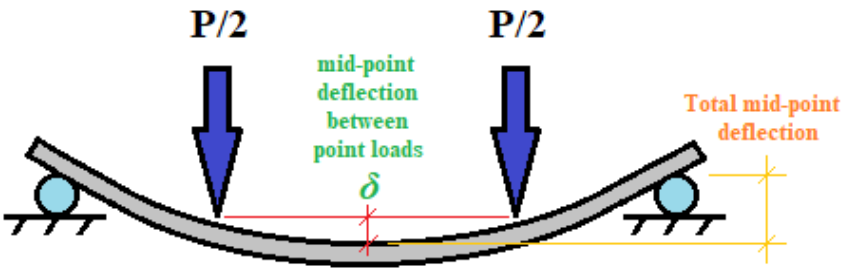

Fig 4.1: *Sketch of how mid-point deflection is defined.*

After initial cracking, the load could be increased in all tests, except for one specimen with the mesh in 45°. The maximum load was higher for specimens with two layers than for the specimens with one layer, and also higher for Type 2 mesh than for Type 1 mesh. A brittle failure with rapture of the textile took place in tests with the mesh in 0°, and a "somewhat ductile behaviour" in form of pull-out of the bundles occurred in tests with the mesh in 45°.

The cracking process could in all tests be followed in detail by the DIC. The crack pattern of the specimens is described for each group of specimens in respective chapter.

Table 4.1: *Overview of maximum load and mid-point deflection between point loads.*

Specimen	Maximum load [N]	Maximum deflection [mm]	Failure
S1-2	1203.0	9.33	Brittle
S1-3	1011.0	9.86	Brittle
S1-4	915.0	10.48	Brittle
S1-45-1	806.3	8.58	Pull-out
S1-45-3	604.7	11.61	Pull-out
S2-45-3	1999.6	6.51	Pull-out
S2-45-4	1778.9	4.85	Pull-out
S1-T1	1564.5	5.88	Combined
S1-T2	1423.7	6.21	Combined

4.2 One layer 0°

For the slabs with one layer 0°, specimen S1-2, S1-3, and S1-4 the results were similar, see **Fig 4.2** and **Figs 4.4-6**. All specimens showed about the same stiffness in the beginning and had a similar and even load increase and crack propagation up to failure. The maximum load was similar for S1-3 and S1-4, around 900 - 1000 N, but slightly higher for S1-2: 1200 N. This was slightly surprising, since specimen S1-2 looked worse visually than the other two which looked flawless, see **Fig 4.3**.

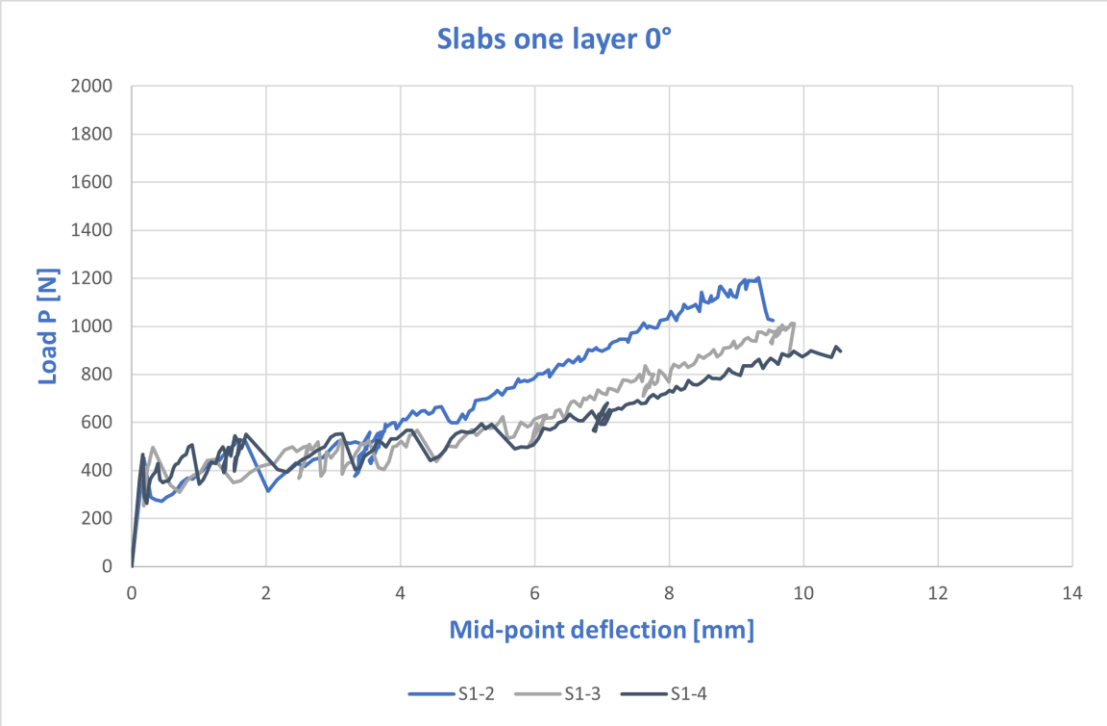

Fig 4.2: *Load and mid-point deflection relation for slabs with one layer in 0° orientation, (Type 1 mesh).*

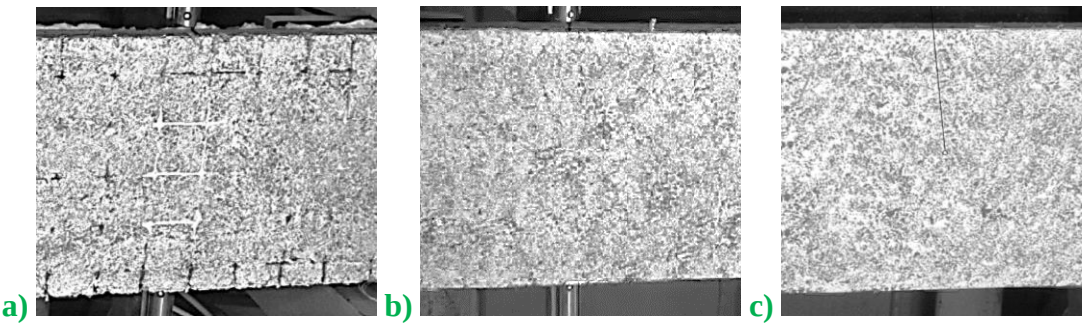

Fig 4.3: *Appearance of specimens, a) S1-2, b) S1-3, and c) S1-4.*

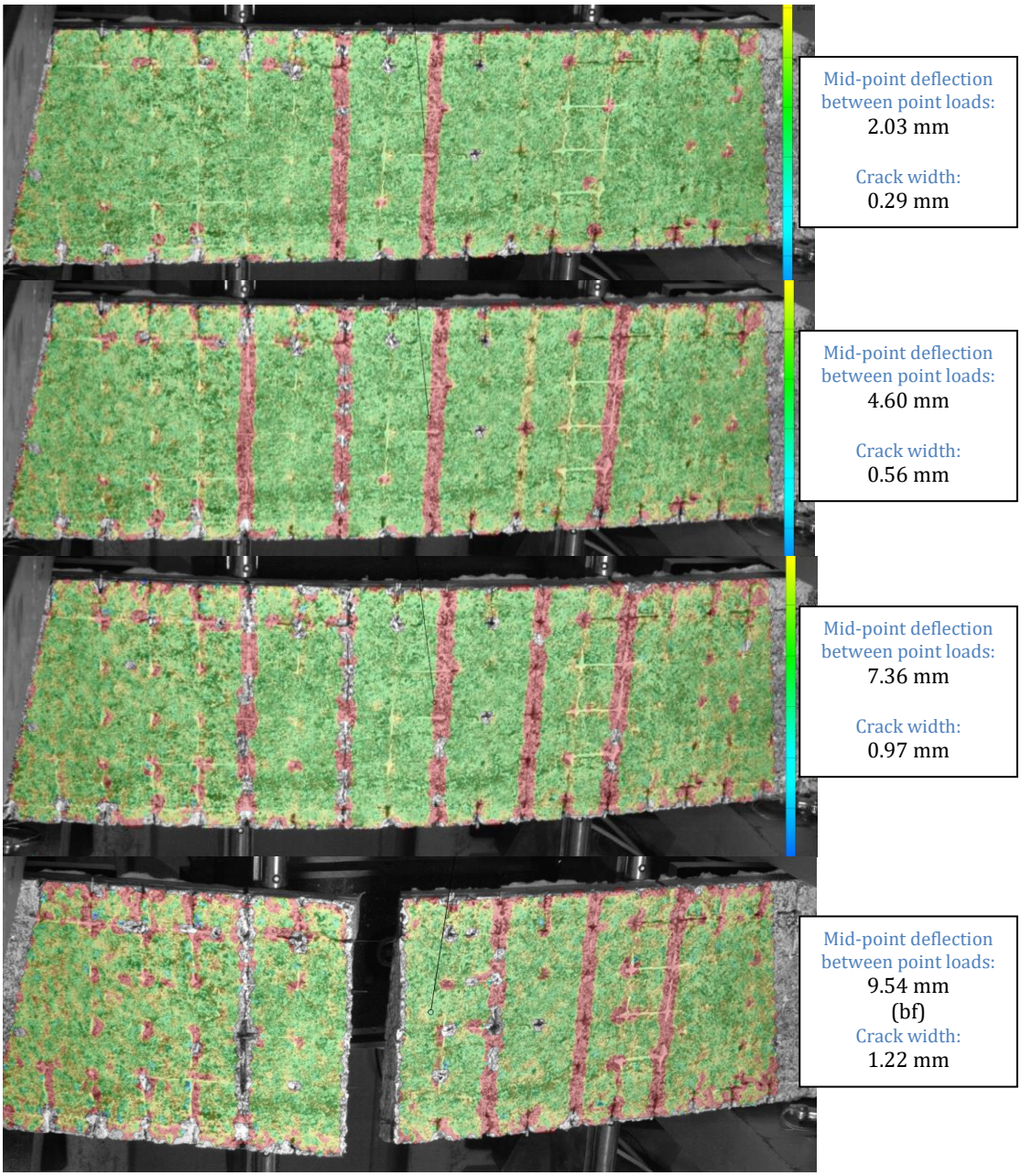

Fig 4.4: *Crack propagation of specimen S1-2, early, middle, late, and at failure (from above).*

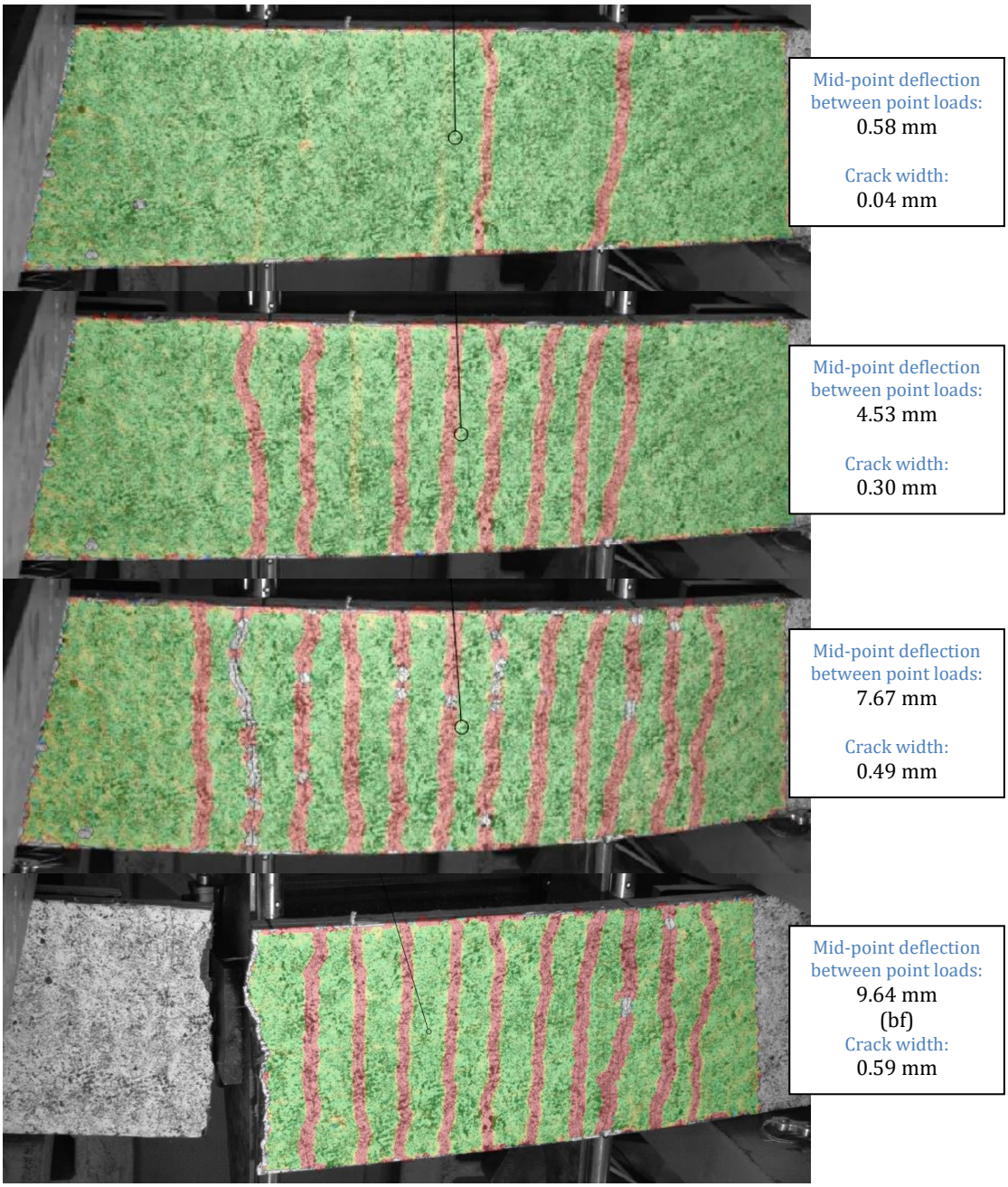

Fig 4.5: *Crack propagation of specimen S1-3, early, middle, late, and at failure (from above).*

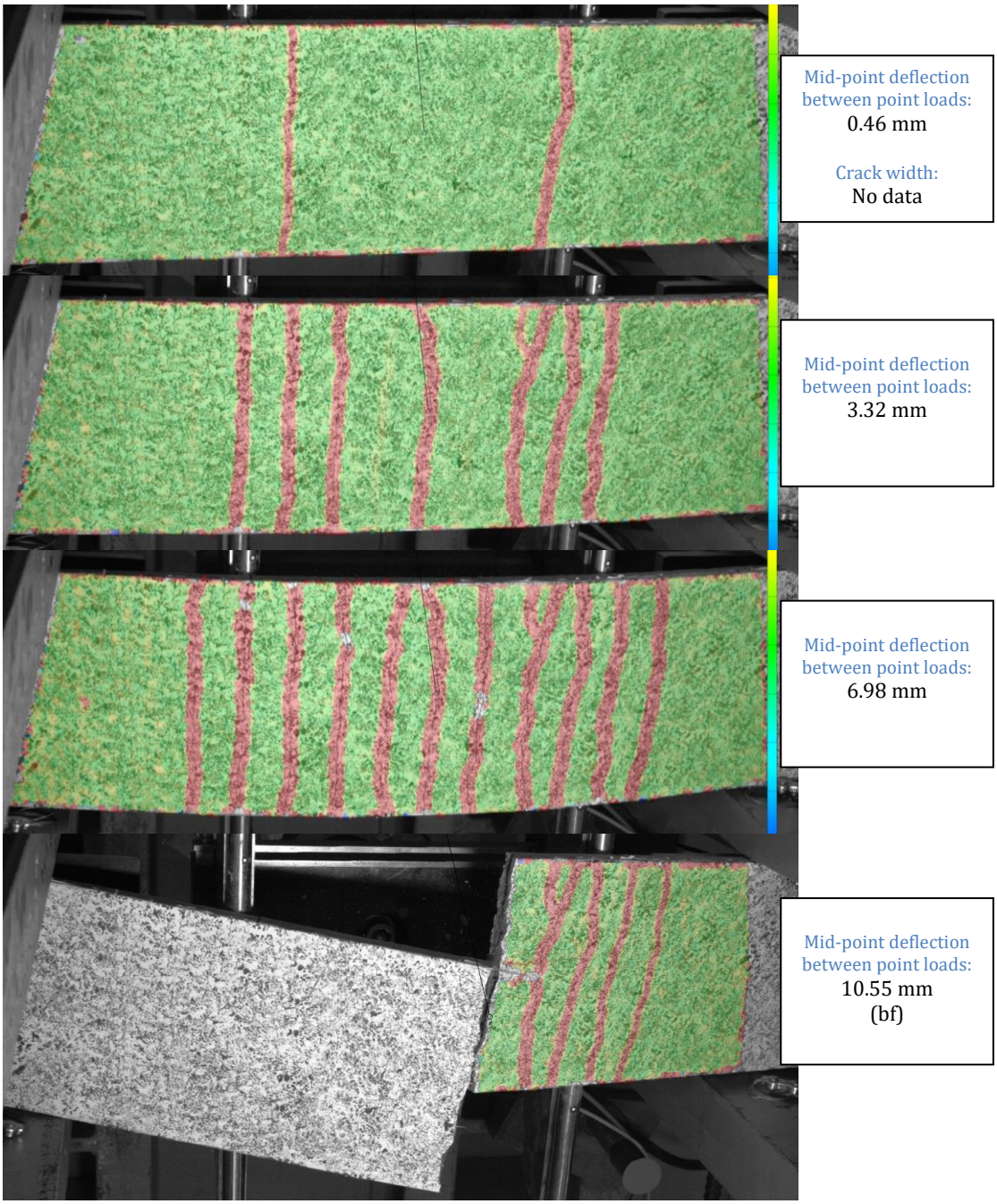

Fig 4.6: *Crack propagation of specimen S1-4, early, middle, late, and at failure (from above).*

4.3 One layer 45°

For slabs with one layer 45°, S1-45-1 and S1-45-3, the load versus deflection graphs are different. For S1-45-1, the maximum load was reached already when the first crack occurred; i.e. the load could not be increased after this point, see **Fig 4.7**. This is most likely due to that the mesh orientation was not aligned with the load direction. S1-45-1 had completely cracked through at deflection 8.58 mm, then it kept on loading until complete pull-out failure at deflection 17.77 mm.

For S1-45-3 there was an initial crack, but it seemed to be able to increase load after cracks appeared, unlike S1-45-1. S1-45-3 also showed a sudden increase in stiffness at a deflection slightly larger than 1 mm. The reason for this increase could not be found; it was noted that there was a measuring point roughly in the middle of this increase. Further, no matter if slightly different point in the DIC measurements were chosen for evaluation of the deformation at the applied loads and in the mid span, a similar behaviour was still evaluated. In both tests, the cracks appeared at the location of the transverse yarns, which can be seen by the "zig-zag" shape of the crack pattern in **Figs 4.8-9**.

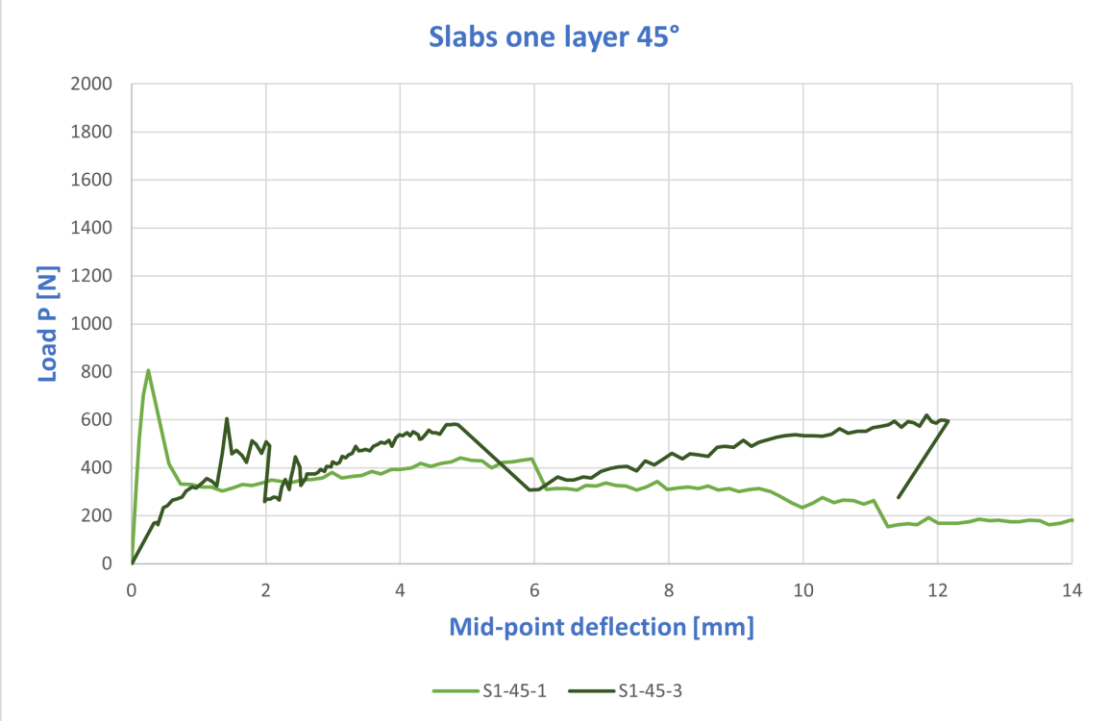

Fig 4.7: *Load and mid-point deflection relation for slabs with one layer in 45° orientation, (Type 1 mesh).*

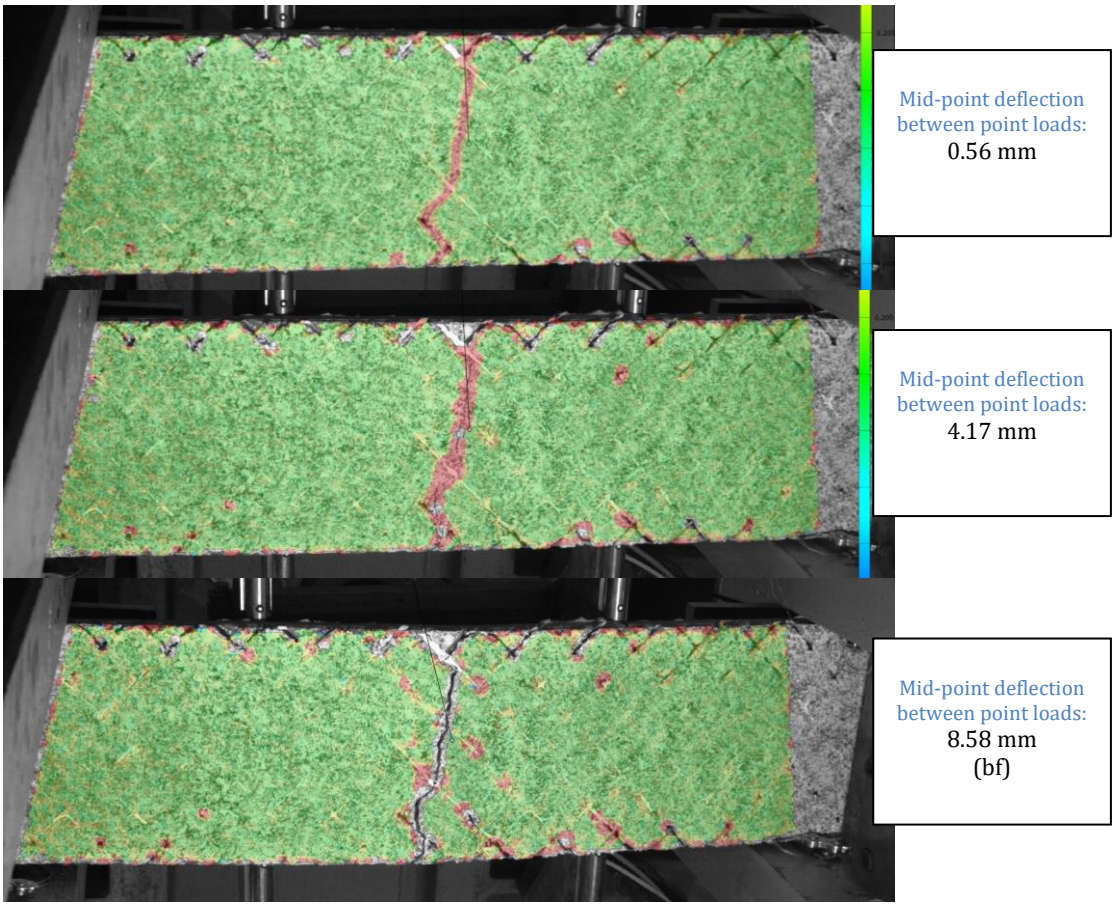

Fig 4.8: *Crack propagation of specimen S1-45-1, early, middle-late, and at failure (from above).*

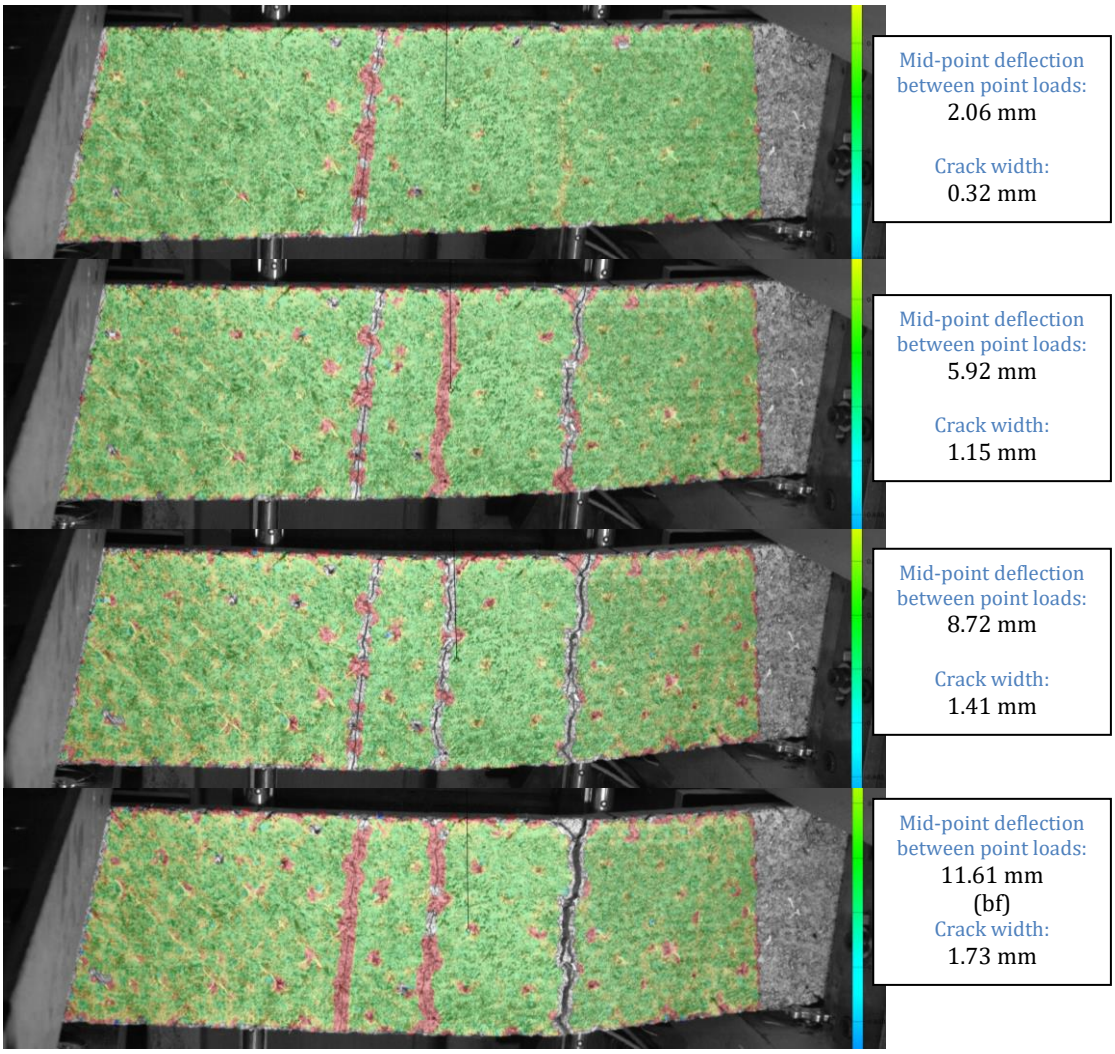

Fig 4.9: *Crack propagation of specimen S1-45-3, early, middle, late, and at failure (from above).*

4.4 Two layers 45°

The slabs with two layers 45°, S2-45-3 and S2-45-4, both show similar behaviour, with a significant higher load than the specimens with one layer, see **Fig 4.10**. This was expected since there is more reinforcement and a thicker cross-section. The load versus deflection graphs also show bigger jumps at cracks, which is probably since the crack must go further into the specimen to activate the second layer of reinforcement. The load increase after the first crack was much higher for S2-45-3, which went from about 1300 N to 2000 N, than for S2-45-4 which went from around 1450 N to 1800 N. S2-45-4 had completely cracked through at deflection 4,98 mm, then it kept increasing load until pull-out failure at deflection 5.81 mm. Also in these tests, the cracks appeared at the location of the transverse yarns, which can clearly be seen by the "zig-zag" shape of the crack patterns in **Figs 4.11-12**.

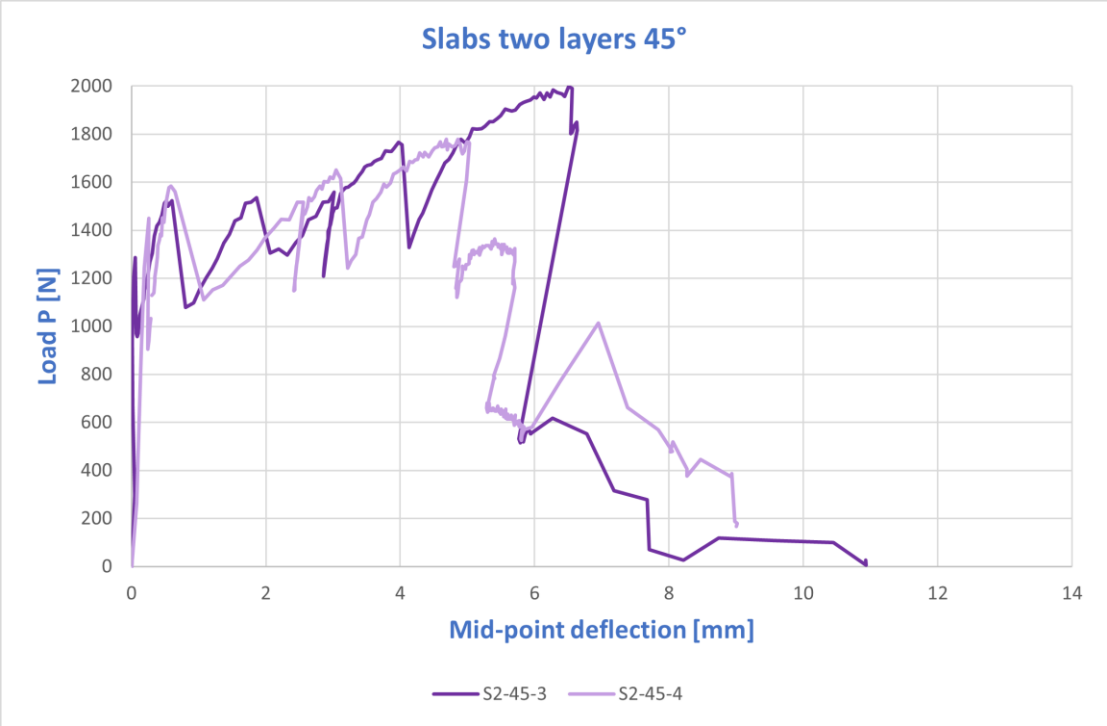

Fig 4.10: *Load and mid-point deflection relation for slabs with two layers in 45° orientation, (Type 1 mesh).*

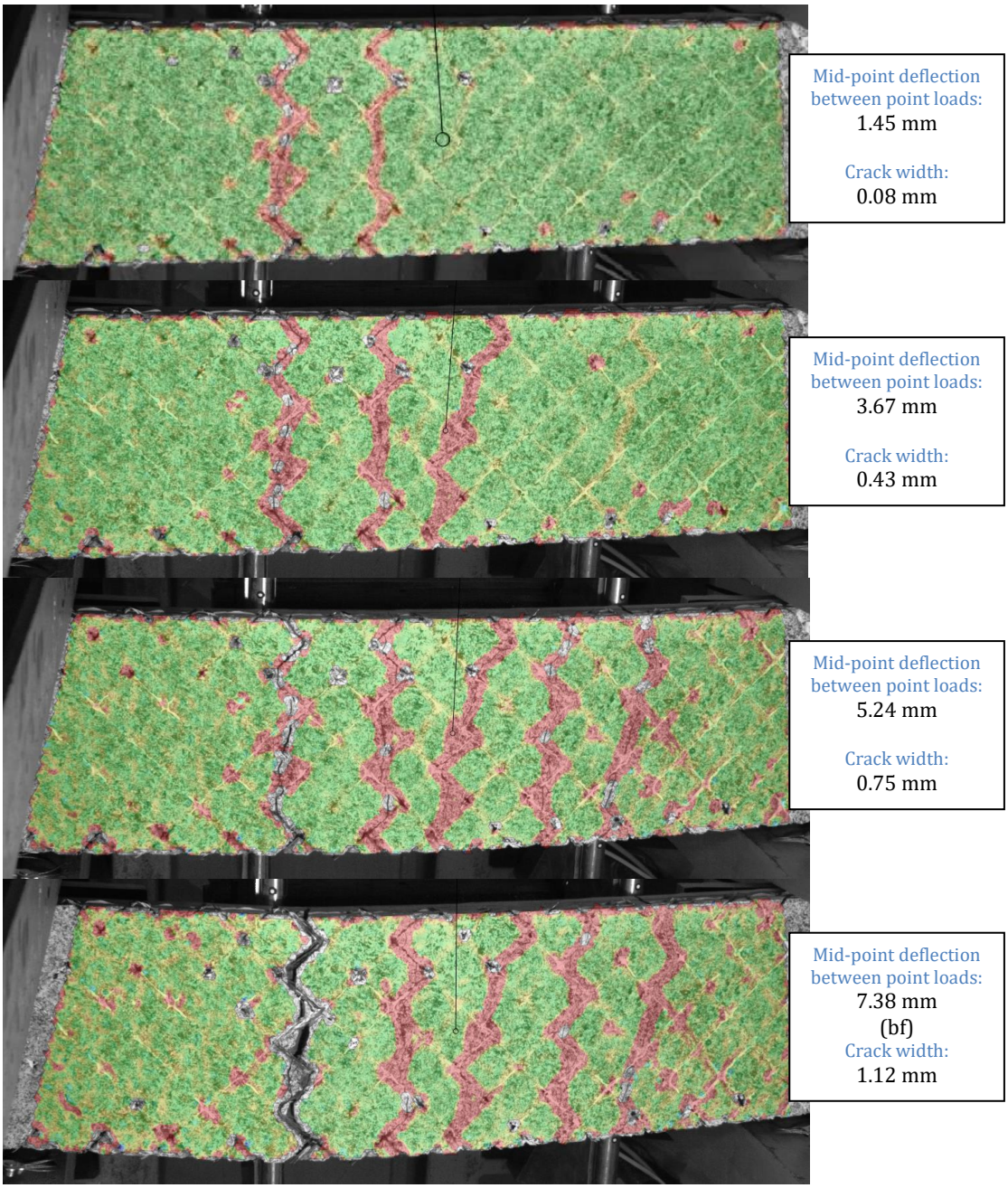

Fig 4.11: *Crack propagation of specimen S2-45-3, early, middle, late, and at failure (from above).*

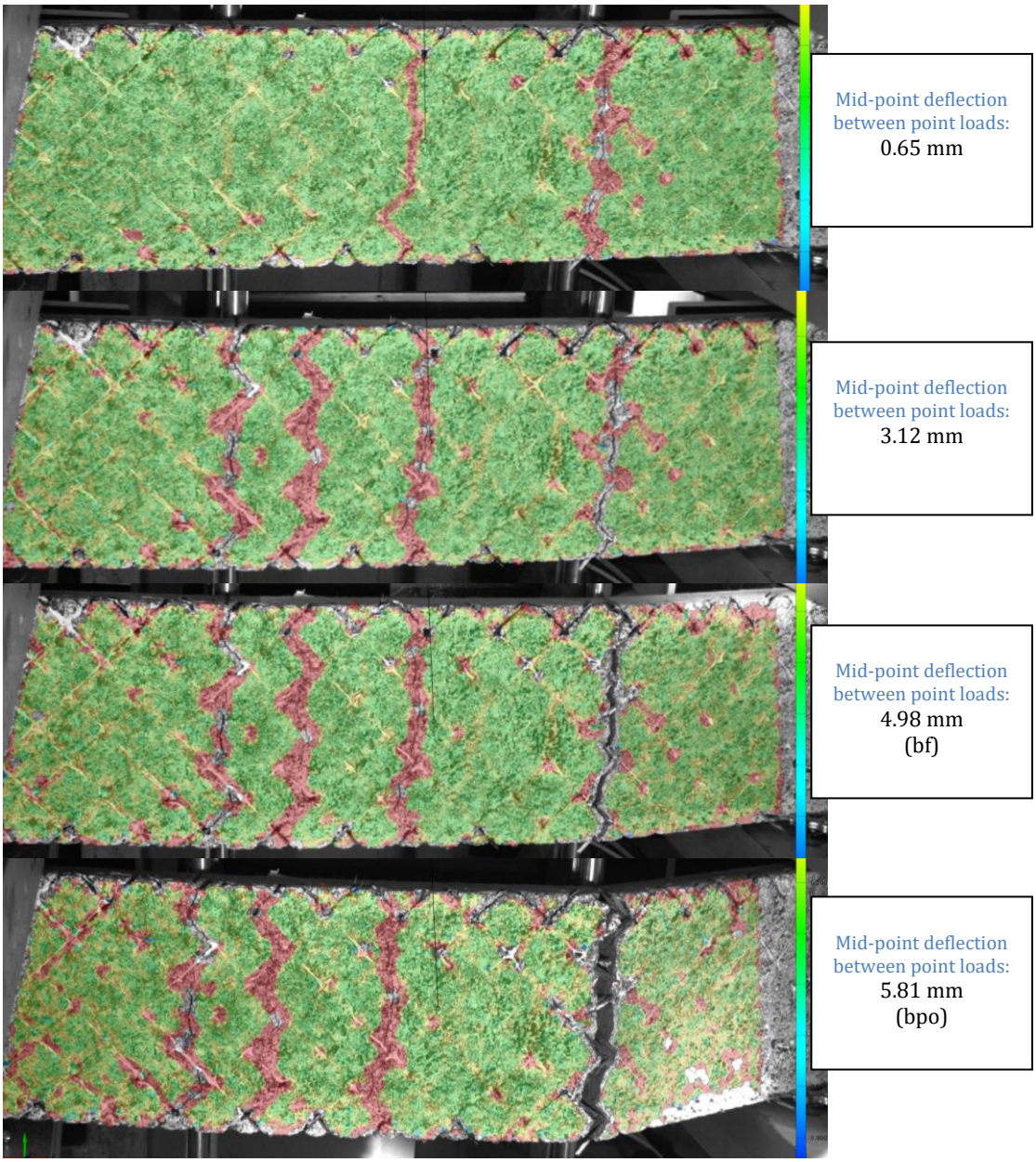

Fig 4.12: *Crack propagation of specimen S2-45-4, early, middle, late, and at failure (from above).*

4.5 One layer 0° Type 2 mesh

For the slabs with one layer 0° with type 2 reinforcement mesh, S1-T1 and S1-T2, the behaviour was roughly similar in terms of load increase and maximum load. Specimen S1-T1 showed higher stiffness than S1-T2, see **Fig 4.13**. Specimen S1-T2 had initial cracks; this could be seen in DIC measurements.

S1-T1 had completely cracked through at deflection 4.95 mm, then it kept increasing load until pull-out failure at deflection 5.80 mm. S1-T2 had completely cracked through at deflection 6.21 mm, then it started sliding (but not increasing load) until pull-out failure.

Both specimens showed a similar crack pattern except for that S1-T2 had more cracks than S1-T1. Otherwise, these two specimens showed similar behaviour, with similar stiffness and maximum load.

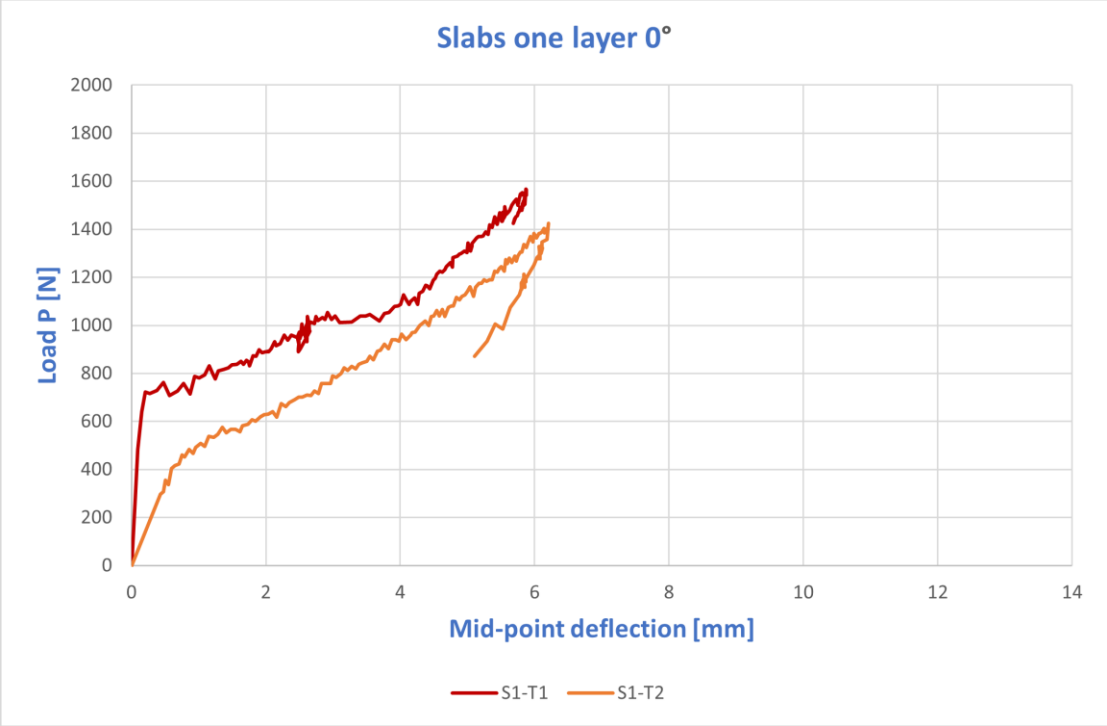

Fig 4.13: *Load and mid-point deflection relation for slabs with one layer in 0° orientation, (Type 2 mesh).*

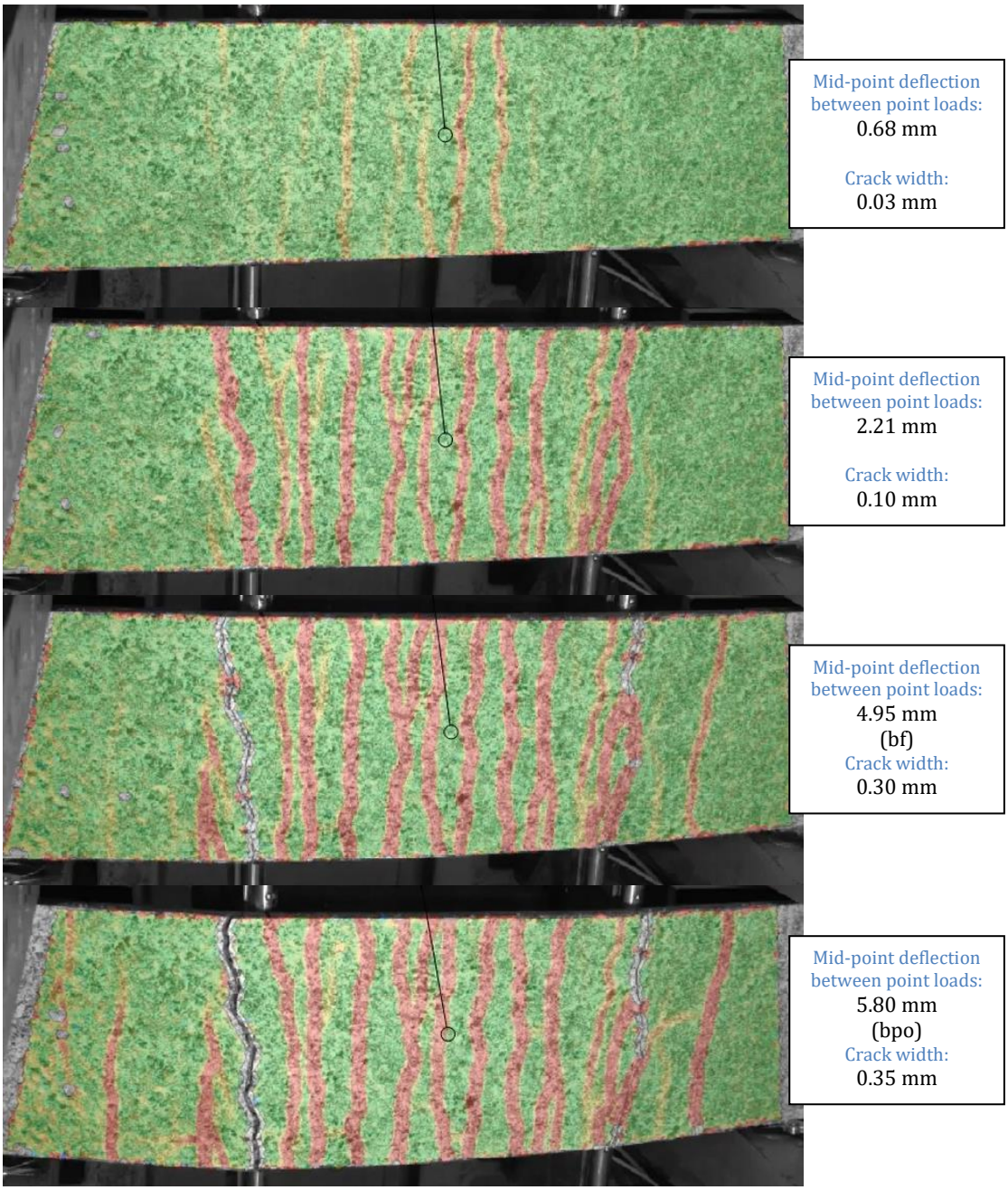

Fig 4.14: *Crack propagation of specimen S1-T1, early, middle, late, and at failure (from above).*

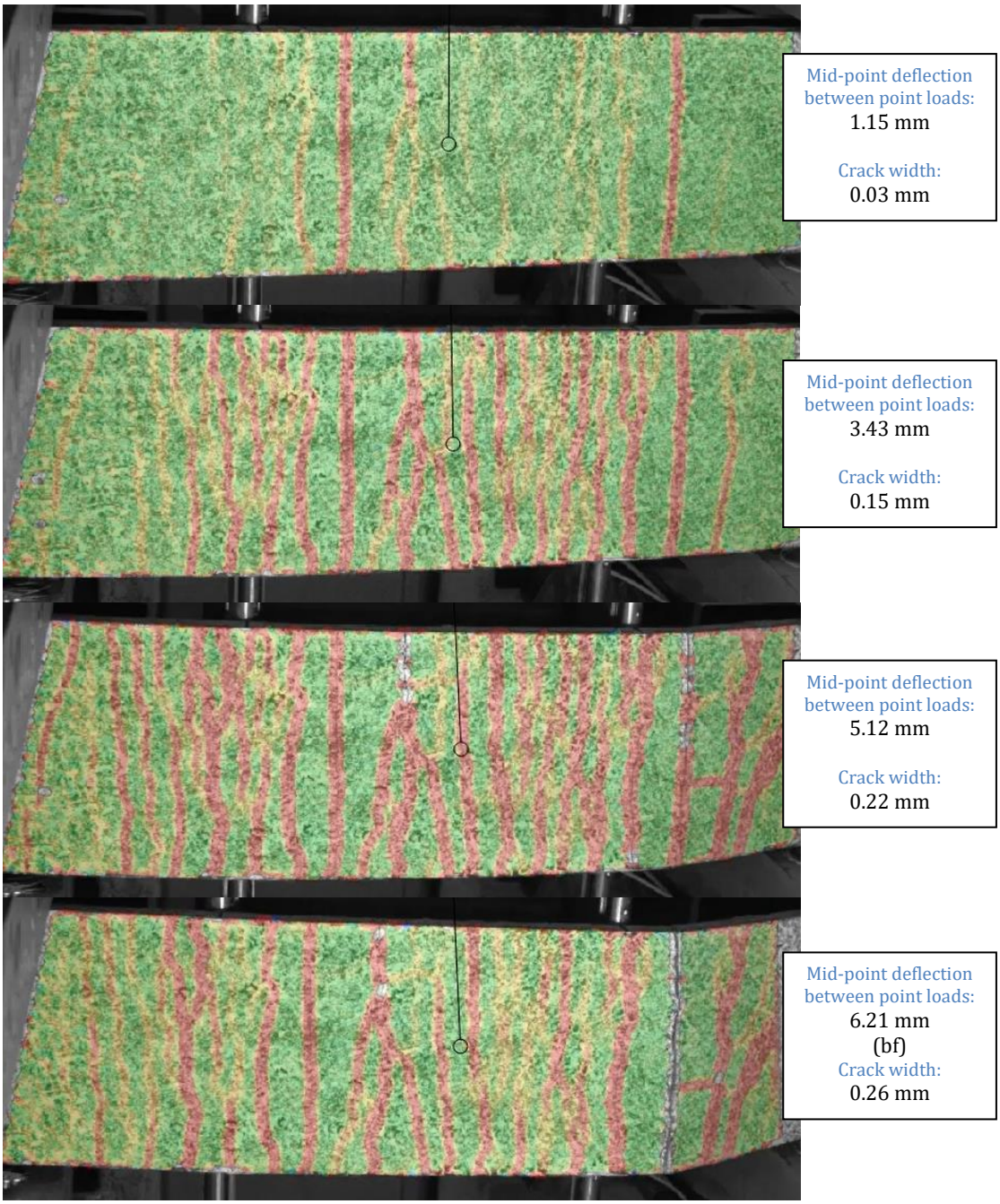

Fig 4.15: *Crack propagation of specimen S1-T2, early, middle, late, and at failure (from above).*

5 Discussion of results

5.1 Load capacity and deflection

The load capacity of the specimens with type 2 mesh was higher than for those with type 1, as seen in Fig 5.1. This was expected since type 2 mesh contains a higher amount of reinforcement in its cross-section. These specimens also showed a smaller deflection at failure compared to all other specimens, and a higher stiffness in the cracked stage. These results may also be explained by the different reinforcement amount. The different production methods may also have contributed; with production method 1 (clamped mesh), there were some difficulties to stretch the mesh. When clamped in the frame, the stiffness of the mesh itself caused it to buckle; this created some "waviness" of the mesh. With method 2 (wet lay-up), the mesh was not "forced" into place, and therefore the mesh was less wavy. This could have influenced the stiffness for S1-2 and S1-3 compared to S1-T1 and S1-T2. Otherwise, they show similar stiffness in the beginning, except for S1-T2 which had initial cracks.

For future work, it would be interesting to study the effect of amount of textile reinforcement in the cross-section.

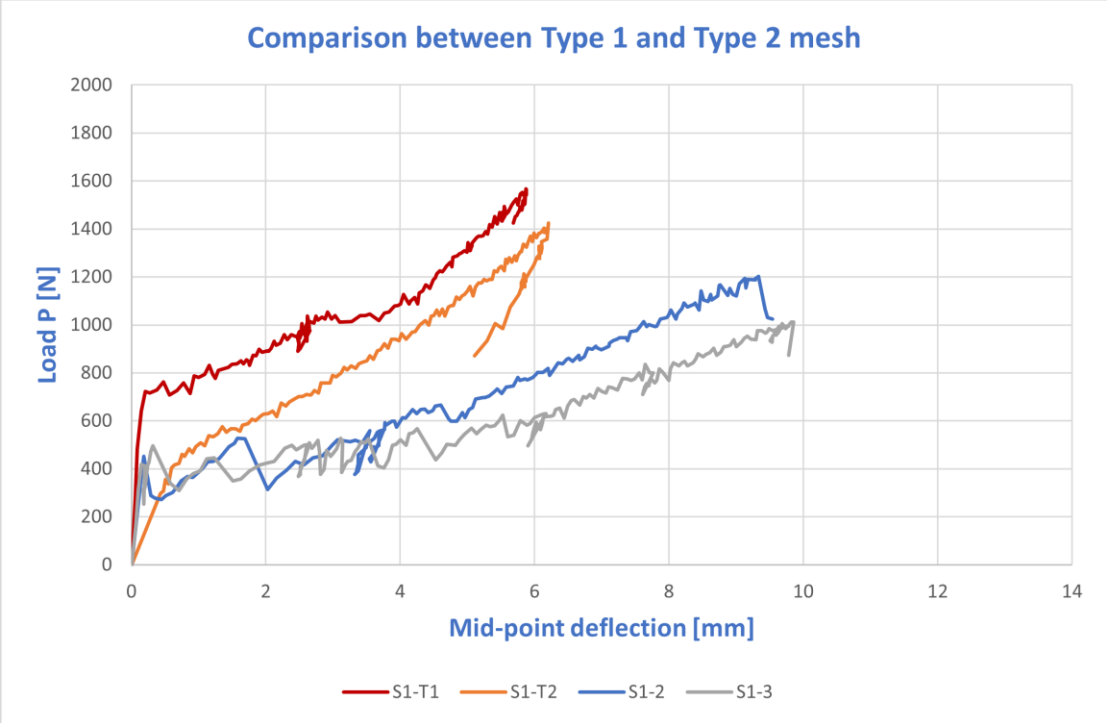

Fig 5.1: *Load and mid-point deflection comparison between Type 1 mesh (S1-2 and S1-3) and Type 2 mesh (S1-T1 and S1-T2).*

5.2 Crack pattern and crack width

The number of cracks in each specimen was studied and showed a large variety among the specimens. Overall, specimens with 45° mesh had fewer cracks than those with 0°. Further, better quality of the specimen resulted in more cracks, see **Table 5.1**.

Table 5.1: *Overview of number of cracks for each specimen.*

Specimen	Number of cracks	Quality of specimen
S1-2	5	Poor
S1-3	12	Good
S1-4	11	Good
S1-45-1	1	Poor
S1-45-3	3	Poor
S2-45-3	5	Poor
S2-45-4	4	Poor
S1-T1	14	Good
S1-T2	23	Good

The transverse yarn showed to be a crack initiator especially for mesh type 1: almost all cracks with this mesh formed right on top of the transverse located yarns; i.e. with a crack spacing of about 40 mm. Specimens with type 2 mesh had a higher number of, and more irregular cracks, not following the mesh structure, see **Fig 5.2**. The type 2 mesh was overall much denser with 112 bundles across and 20 bundles along compared to type 1 with 23 bundles across and 5 bundles along.

For mesh type 1, cracks typically appeared at the location of the transverse yarns, both for 0° and 45° mesh. Especially in the specimens with 45° mesh, this was clearly visible as the cracks showed a “zig-zag” shape following the mesh, see **Figs 4.11-12**.

The slabs with 0° mesh orientation showed more and smaller jumps in the load-deflection curve compared to those with 45° angle, indicating a more evenly distributed and propagating crack pattern up to failure. In the tests with 45°, both with one and two layers, the jumps in the load-deflection curves were much larger at cracking.

In the tests with two layers 45° reinforcement, the specimens could continue to take additional load after cracking; the specimens with one layer in 45° were not capable of that.

a)

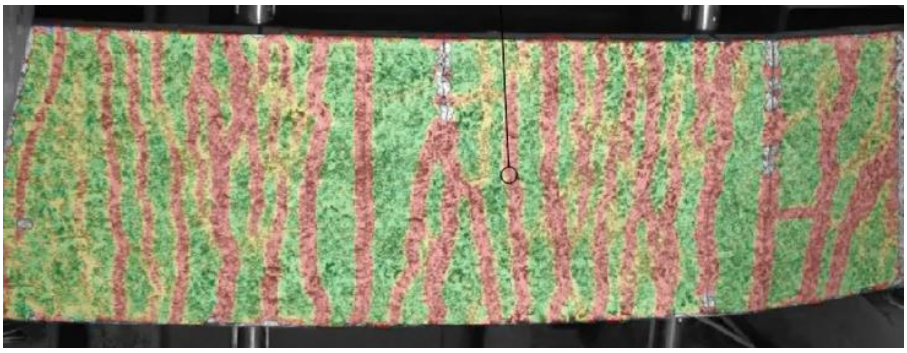

b)

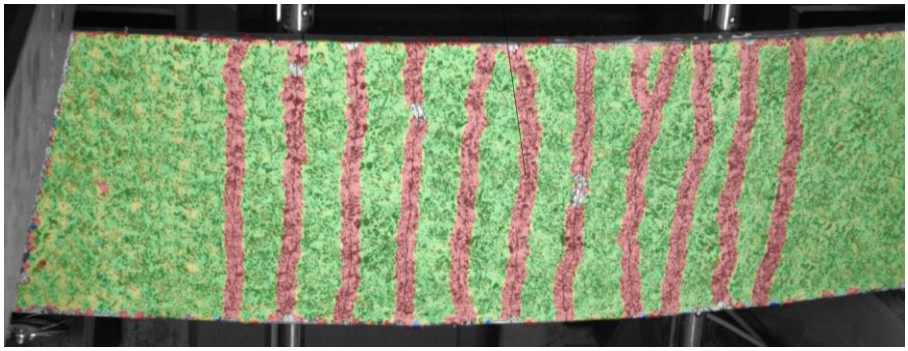

Fig 5.2: *Comparison of crack pattern between meshes, a) specimen S1-T2 with Type 2 mesh, b) specimen S1-4 with Type 1 mesh.*

The crack width was measured in DIC and is presented as an average crack width of 3 cracks for each specimen. The crack width was much larger for the specimens with 45° oriented mesh in comparison to 0°, see **Fig 5.2**. Specimen S1-3 had about the same crack width and number of cracks as S1-T1. Specimen S1-T2 stands out with a much higher number of cracks, and smaller crack width.

Despite the better performance of specimen S1-2 in terms of higher load capacity and stiffness in cracked stage, it had fewer and larger cracks than specimen S1-3. This indicates that the quality of the specimen and a proper coverage is important.

The individual crack widths in a specimen were similar between the cracks in roughly all specimens with no crack standing out. The propagation was generally even and the ratio between the largest and smallest crack was less than 2.

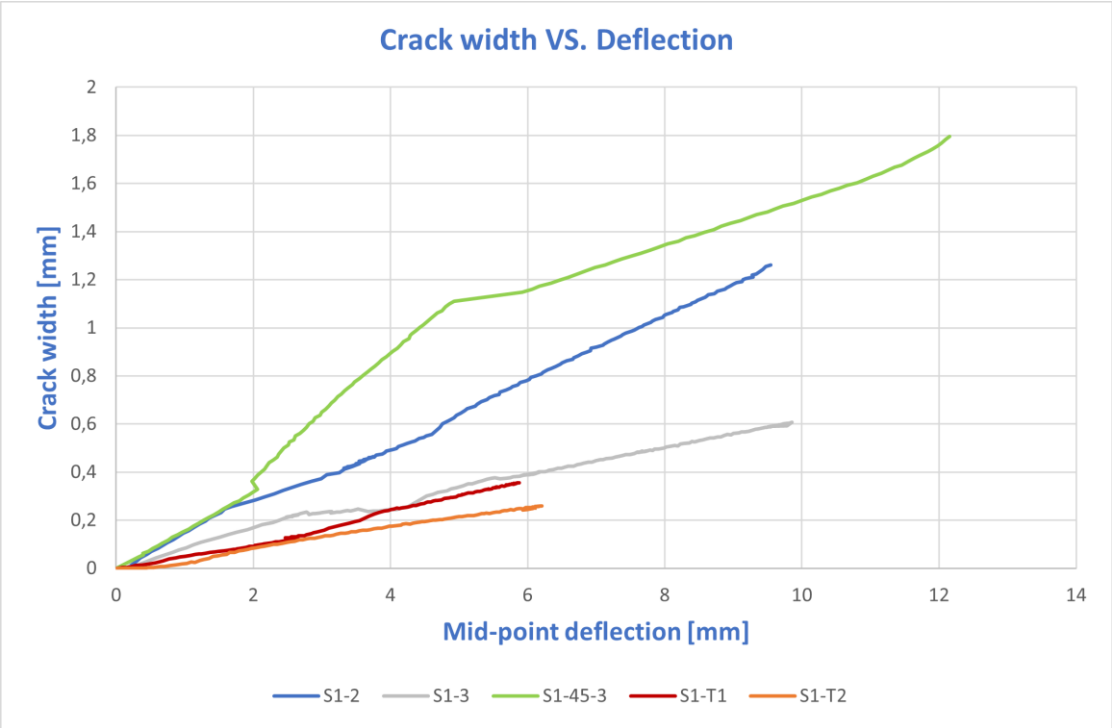

Fig 5.2: Crack width versus mid-point deflection for some of the slabs.

The flexural tensile strength was calculated according to EC 2 as:

$$f_{ctm,fl} = k \times f_{ctm}$$

with $k = 1.6 - \frac{h \times 1000}{1000}$, where **h** is the thickness of slab, and $f_{ctm} = 0.9 \times f_{ct,sp}$ where $f_{ct,sp}$ was taken as the average tensile strength from **Table 3.6**. The expected cracking loads were calculated according to Navier's formula as:

$$\sigma = \frac{M}{I} \times z \qquad \text{rewritten with } W_b = \frac{1}{I} \times z \text{ as:} \qquad \sigma = \frac{M}{W_b}$$

with $\sigma = f_{ctm,fl}$, and W_b is the section modulus ($W_b = \frac{bh^2}{6}$). The total applied load was then calculated as:

$$P = 2 \times \frac{M}{a}$$

where **a** is the distance between point load and support, and $M = W_b \times f_{ctm,fl}$. The calculated cracking load can be found in **Table 5.2**.

The specimens with one layer in 0° all cracked at a lower load than calculated, on average 14.8% lower. For the specimens with 45° that did not have initial cracks, the load at first crack was larger than the calculated value. For the specimens with two layers in 45° the load at cracking was on average 16.6% higher than the calculated value.

Table 5.2: Comparison of cracking loads P and calculated cracking load.

Specimen	Experimental cracking load P [N]	Calculated cracking load P [N]
S1-2	451.1	523.5
S1-3	419.1	
S1-4	467.1	
S1-45-1	806.3	
S1-45-3	Initial crack	
S2-45-3	1286.2	1173.3
S2-45-4	1449.3	

5.3 Utilization factor

To investigate how well the tensile strength of the textiles was utilized, the utilization factors from literature, 0.2 and 0.52 (Voss, 2006), were multiplied to the assumed tensile capacity for the carbon fibre; which was 5500 N for one bundle. The load capacity was calculated from moment equilibrium as:

$$\mathbf{P = 2 \times \frac{M}{a}}$$

where **a** is the distance between the point load and support, $\mathbf{M = F_{cf} \times z}$, with **z** as the inner leaver arm of the cross-section; assumed to be 90% of the thickness of the slab reduced with the average distance to the reinforcement from the bottom. The force $\mathbf{F_{cf}}$ was calculated as:

$$\mathbf{F_{cf} = C_{uf} \times f_{fn} \times n_{lay} \times n_{bun}}$$

where $\mathbf{C_{uf}}$ is the utilization factor (0.2 or 0.52), $\mathbf{f_{fn}}$ = 5500 N , $\mathbf{n_{lay}}$ is the number of layers in the cross-section, and $\mathbf{n_{bun}}$ is the number of bundles in the cross-section. Comparisons can be seen in **Table 5.3**.

Table 5.3: Comparison of maximum loads P and utilization factor.

Specimen	Experimental max load P [N]	Utilization factor	Calculated max load P [N] for factor 0.2	Calculated max load P [N] for factor 0.52
S1-2	1203.0	0.40	594.0	1544.4
S1-3	1011.0	0.34		
S1-4	915.0	0.38		
S1-45-1	806.3	0.31		
S1-45-3	604.7	0.20		
S2-45-3	1999.6	0.22	1782.0	4633.2
S2-45-4	1778.9	0.20		

The utilization factor showed to be roughly in between the values from literature, 0.2 and 0.52, see **Table 5.3**. For specimens with 0° orientation mesh, the average was 0.37, while it was much lower for specimens with 45°, 0.23. This was expected since the reinforcement in the 45° specimens is not oriented in the load direction, and thus is less efficient.

Strength loss in carbon reinforcement can undermine the usability, especially for freeform shapes where the reinforcement will not always be placed in the load direction. However, TRC is still considered to be a promising solution, since the tensile strength is still more than double of that of traditional B500 steel used today, and also considering the other benefits like corrosion resistance. This means that the utilization factor becomes an important design parameter to consider and improve to make TRC-structures more competitive.

5.4 Mesh orientation

As described, specimens with 45° reinforcement orientation had lower load capacity and fewer cracks with larger crack widths compared to specimens with 0°. Further, the specimens with 45° reinforcement in one layer showed no load increase after first cracking. These are all major drawbacks of a disoriented mesh, which may make it difficult to justify its usefulness. However, it is worth to point out that the 45° specimens had substantially larger deformation capacity than 0°.

It is also worth to note that the fewer and larger cracks may be related with the poor quality of 45° the specimens; specimen S1-2 with mesh in 0° and poor quality also had fewer and larger cracks (see **Table 5.1**).

5.5 Manufacturing method

The framework manufacturing method 1, with clamped mesh, took quite some time in comparison to method 2, wet lay-up, but each method has its advantages. With a clamped mesh, it is possible to control the exact positioning of the mesh in the specimen and it is preferable for multilayer reinforcement. Another advantage for laboratory specimens is that it is possible to let the mesh stick out from the side of the specimen to be able to see the exact location of the mesh after casting. However, the disadvantages are that it is more time consuming, and it showed some difficulties to stretch the mesh. When clamped in the frame, the stiffness of the mesh itself caused it to buckle and create some “waviness” of the mesh. Small displacements of the plastic frame when screwed together created forces in mesh causing it to buckle. In some specimens the mesh got “wavy”, and this could have influenced the results due to the reinforcements orientation in relation to load direction. In method 2 (wet lay-up) in the other hand, the mesh was not “forced” into place, and therefore did not have this problem.

Method 2, wet lay-up, is much quicker and it is easier to produce the specimens. It is also certified that the mesh is properly covered with concrete, and the mesh does not buckle since it is not “forced” in position, as from clamping. However, it is much harder to control the exact height and/or distance between meshes since this requires a meticulous smoothening of the first layer of concrete. Even if a smooth surface is

achieved, application of a second layer can modify the exact location of the first layer. For laboratory specimens, it is also a disadvantage that it is not possible to visually locate the mesh position afterwards, unless markings are made.

The problems from casting due to the poor pourability of the concrete led to that the mesh was not covered properly, as seen in the discarded specimens (**Fig 3.5**). This is a very important aspect since the force transfer between the concrete and the reinforcement is essential for these structures. Also, the concrete cylinders for the compression tests had air bubbles, despite being carefully vibrated. They are therefore expected to have lower strength results compared to specimens of proper quality.

The concrete was supposed to be "pourable", so it was expected to flow easily and cover the yarns and spread out and fill out the specimens properly at casting. Based on the results of this work, it is highly recommended to test the flowability of the concrete before casting.

6 Conclusions

6.1 General conclusions

Four-point bending tests of one-way carbon fibre reinforcement slabs were executed. Specimens were produced with different types of reinforcement mesh, and one of the types in two different orientations: 0° and 45° angle. Load versus deflection were studied as well as crack pattern and crack width.

Planning and manufacturing took some more time than expected, but the execution of the experiments went almost flawless. However, great care and precision when handling the specimens is advised to avoid initial cracks.

The rig set-up for the four-point bending test was custom made for this thesis work. DIC was used and was the reason to build the set-up upside down to be able to direct the cameras on the tensile side of the specimens. This was also a good way to be able to visually see and follow the testing process.

Two manufacturing methods were used: clamped mesh (method 1) and wet lay-up (method 2). Both methods have its own advantages and disadvantages, but can both be handled depending on how well the precision of the execution is. In both methods, it is of high importance to get the concrete mix flowable enough to achieve full coverage of the reinforcement; this showed to be problematic in the method with clamped mesh, which led to that many of these specimens had to be discarded. Overall, the choice of manufacturing method is mostly a matter of time spent and what is considered most important.

From the tests, clear differences between 0° and 45° reinforcement mesh was found in both load, deformation, crack pattern and crack width, as well as failure mode. Generally, specimens with mesh placed in the load direction were able to carry more load, had smaller deflection and resulted in brittle failure with rupture of the textile. For specimens with an angled mesh, cracks were more severe, but the specimens had higher deflection capacity and their failure mode was a less brittle pull-out failure. It should be noted though, that all specimens with angled mesh had poor casting quality, so future investigations are needed.

In regard of crack appearance, the number of cracks in each specimen was studied and showed some variety among the specimens. Overall, specimens with 45° mesh had fewer cracks than those with 0°. The transverse yarn showed to be a crack initiator especially for mesh type 1: almost all cracks with this mesh formed right on top of the transverse yarns; this was clearly visible in the specimens with 45° mesh as the cracks showed a “zig-zag” shape. Specimens with type 2 mesh had a higher number of, and more irregular cracks, not following the mesh structure. Further, better quality of the specimen resulted in more cracks.

A variety of specimens with reinforcements mesh in both 0° and 45° orientation were tested and thereby provide data regarding the structural behaviour in bending. Experience regarding manufacturing method, planning and execution of this kind of test has been gained and the results will be of use in further studies, including modelling.

6.2 Suggestions for further work

The rig set-up for the four-point bending test was custom made for this thesis and was built upside down to be able to direct the cameras (for DIC) on the tensile side of the specimens. This setup showed to work very well, and is recommended for use in further studies, as it is a good way to be able to visually see and follow the testing process, and also to protect the camera equipment from falling parts.

For future work, it would be interesting to study the effect of amount of textile reinforcement in the cross-section, since these results varied a lot, to see a relation between load capacity and amount of reinforcement. Also, since the transverse yarns showed to be a crack initiator, it would be useful to study different layouts of textile reinforcement meshes.

The results from the specimens with angled mesh showed larger cracks and lower load capacity in regard of utilization factor, but they all were also of poor quality. Therefore, further studies to investigate angled mesh with specimens of proper quality is needed. With regard of the challenges to have the reinforcement in the load direction, it would also be interesting to study the difference between FRC, where there are always fibres in all directions, and TRC in both two-way slabs and freeform structures.

7 References

Al-Emrani M. and Engström B. and Johansson M. and Johansson P. (2013): *Bärande konstruktioner Del 1*. Institutionen för Bygg- och miljöteknik, Avdelning för konstruktionsteknik, Chalmers tekniska högskola, Göteborg, Sverige, 2013, pp. B211-B229.

Al-Emrani M. and Engström B. and Johansson M. and Johansson P. (2011): *Bärande konstruktioner Del 2*. Institutionen för Bygg- och miljöteknik, Avdelning för konstruktionsteknik, Chalmers tekniska högskola, Göteborg, Sverige, 2011, pp. B31-B45.

Budds, D. (2019): How do buildings contribute to climate change?. Curbed, 19-09-2019. Retrieved 2021-06-01 from: https://www.curbed.com/2019/9/19/20874234/buildings-carbon-emissions-climate-change

Delibastic A. and Havatleh R. (2019): *Tunna textilarmerade betongplattor: Provmetod för belastning i planet*. Bachelor's thesis ACEX20-19-27, Institutionen för arkitektur och samhällsbyggnadsteknik, Avdelning för konstruktionsteknik, Betongbyggnad, Chalmers tekniska högskola, Göteborg, Sverige.

Engström B. (2014): *Design and analysis of slabs and flat slabs*. Report 2011-5, Department of Civil and Environmental Engineering, Division of Structural Engineering, Concrete Structures, Chalmers University of Technology, Göteborg, Sweden, 2014.

European committee for standardization (2004): *Eurocode 2: Design of concrete structures*. Retrieved 2021-06-01 from https://www.phd.eng.br/wp-content/uploads/2015/12/en.1992.1.1.2004.pdf

GOM GmbH. ARAMIS Adjustable. Retrieved 2021-06-01 from: https://www.gom.com/metrology-systems/aramis/aramis-adjustable.html

GOM GmbH. GOM Correlate. Retrieved 2021-06-01 from: https://www.gom.com/3d-software/gom-correlate.html

Hegger J. and Voss S. (2008): Investigations on the bearing behaviour and application potential of textile reinforced concrete. *Engineering Structures*, Volume 30, Issue 7, July 2008, Pages 2050-2056, 1st International Conference Textile Reinforced Concrete (ICTRC), Institute of Structural Concrete, RWTH Aachen University, Germany, 2006, pp. 151-160, Retrieved 2021-06-01 from: https://www.sciencedirect.com/science/article/pii/S0141029608000126

Hegger J. and Voss S. (2006): *Dimensioning of textile reinforced concrete structures*. 1st International Conference Textile Reinforced Concrete (ICTRC), Institute of Structural Concrete, RWTH Aachen University, Germany, RILEM Publications SARL, 2006, pp. 151-160.

Lundgren K. (2017): *Textilarmering*. Chapter 7.6 in Betonghandbok Material, Del 1, Svensk Byggtjänst 2017.

Mobasher B. (2012): *Mechanics of fiber and textile reinforced cement composites*. International Standard Book Number-13: 978-1-4398-0661-6 (eBook - PDF), CRC Press, Taylor & Francis Group, London, 2012.

May S. and Steinbock O. and Michler H. and Curbach M. (2019): Precast Slab Structures Made of Carbon Reinforced Concrete. *Structures*, Volume 18, April 2019, Pages 20-27, Retrieved 2021-06-01 from: www.elsevier.com/locate/structures

Portal N. and Thrane L. and Lundgren K. (2015): *Flexural Behaviour of Textile Reinforced Concrete Composites: Experimental and Numerical Evaluation*. Artikel i vetenskaplig tidskrift, 2017, CBI Swedish Cement and Concrete Research Institute, Borås, Sweden and Department of Civil and Environmental Engineering – Structural Engineering, Chalmers University of Technology, Gothenburg, Sweden, 2015.

Roodman D. and M. Lenssen N. and Peterson J. (1995): *Worldwatch Paper 124: A Building Revolution: How Ecology and Health Concerns Are Transforming Construction.* Volym 124 of Basque Studies Program Occasional Papers Series, Volym 124 of Worldwatch paper, ISSN 0270-8019, Worldwatch Institute, Washington, D.C., USA, ISBN 1-878071-25-4.

Sciegaj A. (2020): *Multiscale Modelling of Reinforced Concrete Structure*. Department of Architecture and Civil Engineering, Division of Industrial and Material Science, Chalmers University of Technology, Concrete Structures, Göteborg, Sweden, 2020.

Sto. (2009). StoFRP Grid 1000 C 390. In: Sto. Retrieved 2021-06-01 from: https://datamaster.sto-net.com/webdocs/0000/SDB/T_07800-011_0208_SV_05_01.PDF

Sto. (2015). StoCrete R40. In: Sto. Retrieved 2021-06-01 from: https://datamaster.sto-net.com/webdocs/0000/SDB/T_07693-001_0208_SV_05_01.PDF

Triantafillou T.C. (2016): *Textile Fibre Composites in Civil Engineering*. Woodhead Publishing, Civil and Structural Engineering: Number 60, Elsevier Science & Technology 2016, Chapter 8.

Van Loo M. (2020): *Experimental Study of the Tensile and Pullout Behavior of Textile Reinforced Concrete*. Student project, Department of Architecture and Civil Engineering, Division of Structural Engineering, Concrete structures, Chalmers University of Technology, Göteborg, Sweden, 2020.